Separation & Purification Reviews
Publication details, including instructions for authors and subscription information:
http://www.informaworld.com/smpp/title~content=t713597294

Protein Separation with Flow-Through Chromatography

William E. Collins[a]
[a] Department of Chemical Engineering, Howard University, Washington, DC, USA

To cite this Article Collins, William E.(1997) 'Protein Separation with Flow-Through Chromatography', Separation & Purification Reviews, 26: 2, 215 — 253
To link to this Article: DOI: 10.1080/03602549708014159
URL: http://dx.doi.org/10.1080/03602549708014159

SEPARATION AND PURIFICATION METHODS, 26(2), 215-253 (1997)

PROTEIN SEPARATION WITH FLOW-THROUGH CHROMATOGRAPHY

William E. Collins, Department of Chemical Engineering, Howard University, Washington, DC 20059 USA

INTRODUCTION

Proteins are isolated in the chemical process industries for a wide variety of uses. Isolation and separation are often conducted with chromatography. Conventional chromatography of proteins is often tedious and can suffer from poor efficiency and resolution. There is a well-known tradeoff between resolution and speed[1]. Newer methods of protein chromatography seek to diminish the shortcomings of conventional methods. New methods are presently being investigated for process, preparative, and analytical applications.

Flow-through chromatography is a promising new method of protein separation that decouples resolution and speed. Sought are enhanced resolution, diminished retention time, and on a preparative scale, the processing of larger samples. Recent techniques include variations of conventional chromatography such as displacement, expanded bed, radial, and flow-through configurations. These techniques also include capillary electrophoresis and hollow-fiber membranes. Capillary electrophoresis provides quick, efficient separation and resolution of multiprotein solutions, particularly in immunoassays isolating free antigen and antibody from the antigen-antibody complex[2]. Diffusion limitations on protein ion exchange have been eliminated using the popular diethylamine ligand immobilized on tentacles attached to the pores of hollow-fiber membranes via graft polymerization[3]. The cylindrical geometry of hollow fibers increases resolution[4] compared to conventional particles.

New chromatographic separations of proteins take several forms. For instance, displacement chromatography[5] enhances effluent concentration in the desired proteinaceous solute by displacing it with a low molecular weight solute. Expanded bed chromatography accommodates highly contaminated, intractable feeds. The unclarified, unremediated feed is applied to the bed bottom to adsorb the desired protein solute and displace the bed. After application is finished, flow is reversed, the bed settled, and the protein solute eluted. Averting bed compression via quite low pressure drops, the configuration for radial chromatography uses conventional media, increasing throughput and diminishing retention time[6]. The technique is suited for

process applications displaying promise in immunoaffinity use. Monolithic chromatography beds have found use in ion exchange applications[7]. Woven textile fabric can be rolled and inserted into a column to simulate a continuous phase[8-10], that provides a separation advantage characteristic of flow-through columns. These results suggest that membrane chromatography, in which membranes are immobilized in columns, would display plate heights unaffected by column velocities. This trend is observed at high velocities[8-10].

Flow-through chromatography[1], its principles[11], and applications[12] have all been recently reviewed. The primary characteristic of flow-through chromatography is intraparticle convection. The technique promises reduced retention and exposure times for both preparative and analytical applications. Flow-through, or perfusion, chromatography supplements the diffusive/adsorptive separation mechanism of traditional chromatography with intraparticle convection. Accordingly flow-through chromatography significantly reduces retention time, but maintains resolution and high throughputs. Proteins spend less time on flow-through columns and risk less exposure to denaturing conditions. Sample recovery and yield are increased while products can be analyzed with excellent resolution downstream. Suitable isolation protocols can be developed and perfected quickly, to facilitate scaleup. Many companies like Glaxo, Abbott Labs, Genentech, and Baxter Biotechnology[3] already practice flow-through chromatography in their industrial protein separations. Flow-through chromatography fails to exhibit the tradeoff between resolution and speed displayed by other types of chromatography. This has many benefits for protein separations, which will be covered in this review.

MEDIA COMPOSITION

A pore geometry promoting intraparticle convection classifies flow-through media. Media appropriate for flow-through chromatography must possess outstanding chemical and mechanical stability (Table I). Suitable media can consist of alumina, silica, or even hydroxyapatite[11]. Most often, these media are based upon beads of a poly(styrene-*co*-divinylbenzene) copolymer (PSDVB). A wider fractionation range is obtained with poly(vinylphenol-*co*-divinylbenzene) copolymer[13], which has broader exclusion limits, but lower selectivity. PSDVB materials have been in use for over 40 years though specific variations of the different pore properties and derivatization have changed over the years[12].

PSDVB Flow-Through Chemistry

The PSDVB particles comprising PerSeptive's POROS flow-through media are synthesized via staged templated suspension polymerization[12]. A crosslinked hydrophilic fimbriated phase is adsorbed to the PSDVB surface to decrease solvent equilibration time and particle shrinking or swelling. Moreover this phase can be readily functionalized to support diverse types of chromatography. The POROS media are stable in 5 N NaOH, 1 N KOH, 1 N HCl, 1% phosphoric acid, 10-60% formic acid, and 100% polar organic solvents. POROS is stable for pH 2-12, unlike HPLC silicas, which degrade at pH > 9 and exhibit cation exchange effects from

TABLE I: COMMERCIAL LARGE-PORE HPLC PACKING MATERIALS

MATRIX	BRAND	PORE DIAMETER (Å)
Polymeric	POROS, PerSeptive BioSystems	7000
	PL4000, Polymer Labs	4000
	MacroPrep, BioRad	1200
	G6000PW, TosoHaas	6000
	Fractogel, E. Merck	2000
	SOURCE, Pharmacia	8000
	HyperD, BioSepra	unavailable
	Ni-NTA Superflow, Qiagen	unavailable
Silica	Daisogel 2205, Diaso	2000
	Nucleosil, Machery-Nagel	4000
Alumina	Unisphere, Biotage	2500
Hydroxyapatite	HA Type S, Koken Science Int'l	2000
	MacroPrep CHT, BioRad	1000

residual silanols. The particle diameter of these media d_p can suit a given application. Available are 10 (analytical applications requiring the highest resolutions), 20, or 50 (preparative applications with low pressure drop) μm. Furthermore PSDVB can be molded as a continuous stationary phase, or monolith. The polymerization mixture is thus cast into columns, and polymerized, to increase pore diameters and intramedia convection[13].

Fimbriated stationary phases bound to PerSeptive's flow-through media endow them with higher capacity and diversify the available separation mechanism[14]. In the past, fimbriated phases were used to augment the capacity[15] of highly rigid silica particles of 10 μm d_p for HPLC. Despite their high resolution and flowrates, the particles suffered from low capacity[16]. Fimbriated phases increase the adsorbing surface area of PSDVB media. The typical fimbriated phase consists of select block copolymers that are adsorbed to the surfaces of PSDVB media and crosslinked[14]. This phase is ordinarily not applied for reversed-phase applications because the PSDVB is already hydrophobic enough to cause enough separation[17]. The thickness of the adsorbed phase is restricted to 80 Å or less so that diffusion into the pores is not occluded. The copolymers consist of hydrophobic and hydrophilic blocks. The hydrophobic block possesses affinity for the PSDVB surface and adsorbs (Figure 1). The hydrophilic block possess affinity for the mobile phase, forms loops when the copolymer adsorbs, and consists of polyethylene oxide or glyceryl-based polymers. The hydrophilic block is functionalized to support ion exchange, affinity, or hydrophobic interaction chromatography. Functionalization proceeds by reacting epibromohydrin with glycidol and subsequently with sorbitol or boron trifluoride. Alternate functionalization chemistries are available. The epibromohydrin-glycidol-sorbitol product can be CNBr or aldehyde activated to immobilize ligands on the fimbriated phase. In particular, pore size-specific functionalization can be achieved, in

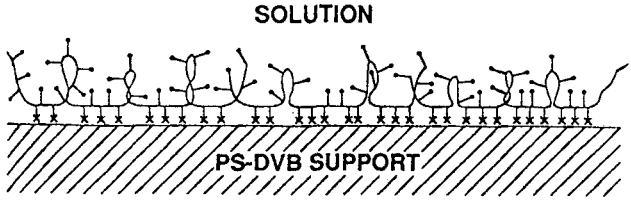

Figure 1. The copolymer coating adsorbed to the PSDVB in order to functionalize flow-through particles. The loops, trains, and tails of the adsorbed coating are shown. X = hydrophobic domains; ● = hydrophilic domains. Reprinted with permission, J. Chromat., 631, 107 (1993). Copyright 1993, Elsevier Publ.

which the diffusive pores are functionalized one way and the throughpores functionalized in another[13]. Thus more than one mode of separation can be realized in the same column, conditions typically unattainable combining media of different single chemistries. These techniques will likely be adapted to synthesize media for metal chelate or thiol exchange chromatography.

There are a number of sources and formulations of PSDVB-based media. Some of these media sizes perhaps possess flow-through capabilities[18]. For example, the media available from Polymer Labs have narrow size distributions of 10, 15, or 25 μm d_p and possess 100, 300, 1000, or 4000 Å pore diameters. The media are suited for ion exchange, reversed phase, and gel filtration chromatography. Media with 1000 or 4000 Å pore diameters suit flow-through applications and exhibit a linear relationship[19] between flowrate and pressure drop up to 3000 psi (21,000 kPa) (Figure 2).

There are alternate configurations of PSDVB media. For example, Pharmacia's SOURCE media[20], though constituted of PSDVB, exhibit a pore-size distribution of 200-10,000 Å, wider than that of the bimodally distributed media of PerSeptive BioSystems. SOURCE media have excellent separation characteristics based upon

A. Proper pore size distribution.
B. Very high pore connectivity of the porous network.
C. Both a very high accessible surface area of the pore network that possesses a high concentration of active sites per unit surface area of the pores.

Thus pore geometry[21] benefits SOURCE[22] and other media (see "Transport Theory") though they are may not flow-through media. Vydac has fabricated VHP particles in 5 or 8 μm d_p from PSDVB for HPLC ion exchange[23]. The HyperD particles of BioSepra[24-27] are available in 10, 20, 35, 60, or 70 μm d_p for ion exchange, affinity, and gel filtration chromatography. These media[25,27] consist of large-pore, highly rigid polystyrene/porous silica matrix permeated by a highly hydrophilic, small-pore hydrogel of modified TrisAcryl.

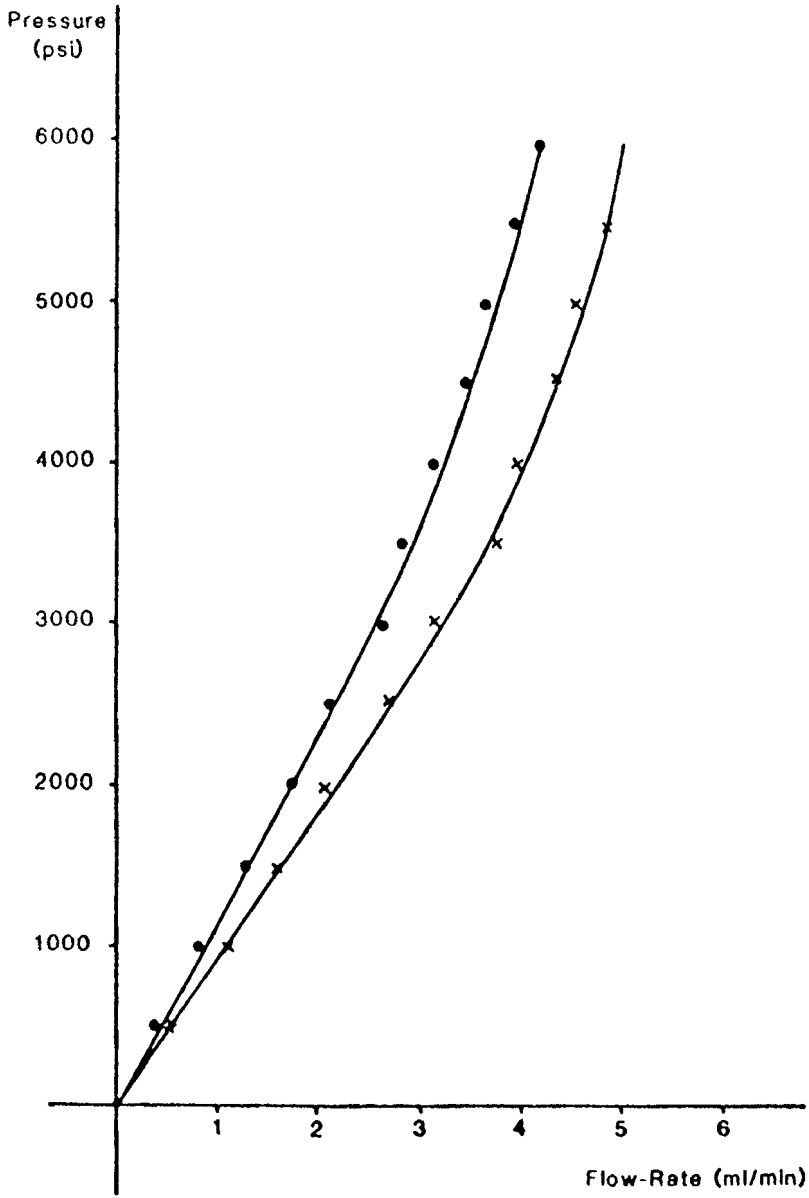

Figure 2. Column pressure vs. flowrate for chromatography at ambient temperature using an eluent of ethanol-water (70: 30, v: v). A 4.6 mm ID x 150 mm column was used with d_p 8 μm. ● = 1000 Å pore diameter; X = 4000 Å pore diameter. Reprinted with permission, J. Chromat., 512, 365 (1990). Copyright 1990, Elsevier Publ.

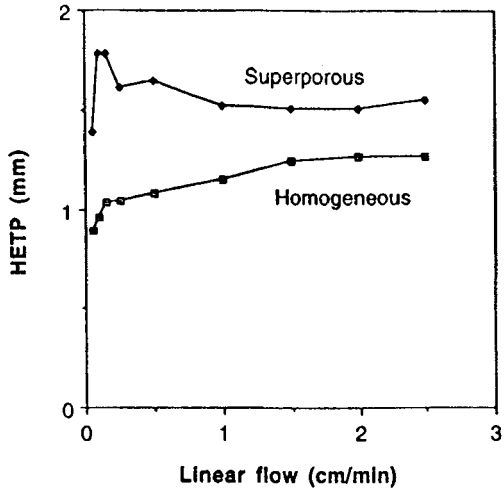

Figure 3. H vs. linear flowrate for size-exclusion chromatography of bovine serum albumin on agarose. A 1.6 mm ID x 150 mm column was used with d_p 400 μm. Reprinted with permission, J. Chromat. A, 734, 231 (1996). Copyright 1996, Elsevier Publ.

Other Flow-Through Chemistries

Flow-through capability is manifested with chemistries other than PSDVB. BioRad has developed its Macro-Prep ceramic hydroxyapatite (M-P CHT) media[28] to facilitate process chromatography. Available in 10, 20, 40, or 80 μm d_p particle sizes, these media are claimed to possess pore diameters of 500-1000 Å, separating proteins via mixed ion exchange. They evince characteristics typical of flow-through chromatography. They display excellent resolution of a number of proteins at the elevated superficial velocity v_0 characteristic of flow-through chromatography. For example, a v_0 of 640 cm/h resolves proteins well for M-P CHT; an upper limit of 1000 cm/h is claimed for v_0. A high column pressure drop ΔP is claimed to leave the resolution of flow-through applications undiminished. A maximum ΔP of 7000 kPa is claimed for M-P CHT particles. These are formed sintering conventional crystals of ceramic hydroxyapatite and are stable in many solvents, including 1% SDS, 2 M NaOH, 8 M urea, acetonitrile, and 100% ethanol.

Qiagen's Ni-NTA Superflow™ media utilize flow-through properties to optimize the chromatography of histidine-tagged proteins[29]. These media consist of 6% agarose heavily cross-linked to withstand ΔP exceeding 1000 kPa plus various corrosive solvents. Particle diameters are 60-160 μm. An upper limit of 3000 cm/h is claimed for v_0.

Recently characterized were agarose particles with a bimodal pore distribution[30]. Synthesized with a double emulsification procedure, these particles possess d_p of 300-500 μm. Moreover they exhibit outstanding promise as flow-through media because

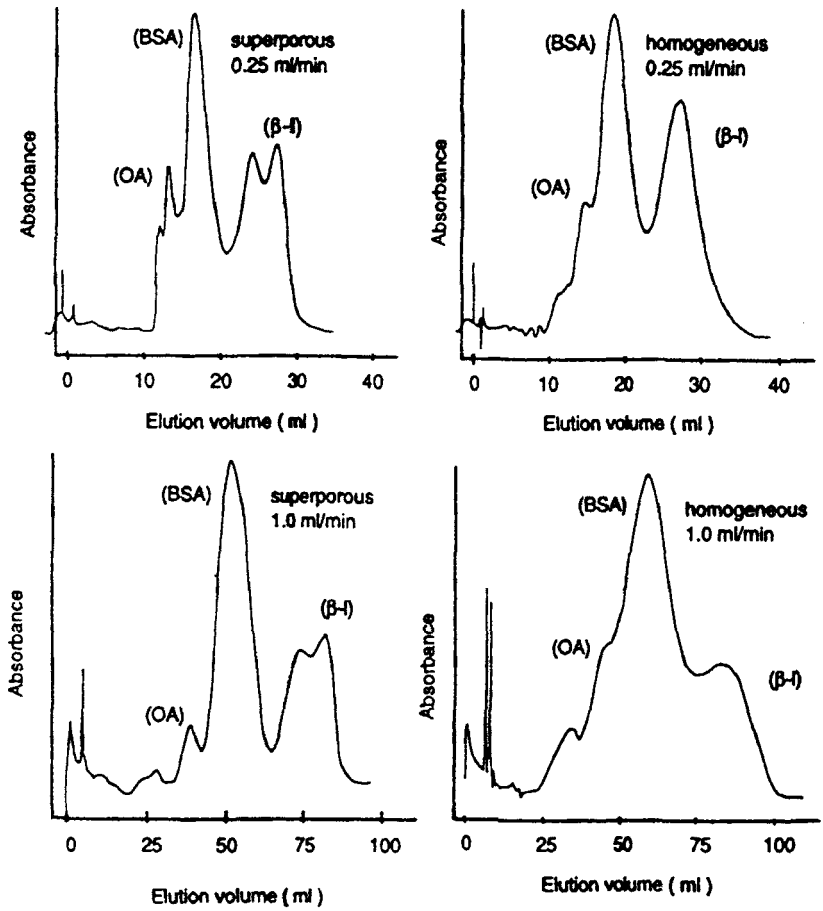

Figure 4. Ion-exchange of homogeneous vs. superporous polyethyleneimine-agarose beads at two elution rates. Chromatography of a 1 ml mixture of bovine serum albumin, ovalbumin, β-lactoglobulin A, and β-lactoglobulin B used a gradient starting with 20 mM Tris-HCl, 0.02 M NaCl, pH 7.0 and ending with 20 mM Tris-HCl, 0.60 M NaCl, pH 7.0 in 100 min. A 5 mm ID x 30 mm column was used with d_p 75-106 μm. Reprinted with permission, J. Chromat. A, 734, 231 (1996). Copyright 1996, Elsevier Publ.

their throughpores possess a diameter of 25-75 μm. For example, water applied to them will pass through without a vacuum. At intermediate and high velocities, H is independent of v_0, unlike agarose particles with homogenous pores, as compared in Figure 3. Polyethyleneimine can coat the superporous agarose particles, adapting them to ion exchange. A standard test of resolution is to apply β-lactoglobulin A

and β-lactoglobulin B, which differ in amino acid composition at only two positions, to candidate media. As shown in Figure 4, the superporous particles resolve the types of β-lactoglobulin, but the homogeneous particles clearly do not.

It is easier to tailor these formulations than some of the very first flow-through formulations. These nonetheless displayed advantageous separation. For example, cabbage alumina was developed in the 1980s, cast into 10 μm microspheres, and coated with polyethyleneimine to be used as chromatography media[8]. The microspheres possessed a leaf structure with 1000-10,000 Å between leaves. Columns of the media were used to separate bovine serum albumin and immunoglobulin G. For superficial velocities of 1-15 cm/min, the height of a theoretical plate was independent of v_0, exhibiting the major attribute of flow-through media, resolution unaffected by speed.

PROPERTIES OF FLOW-THROUGH PARTICLES

Transport efficiency between the mobile and stationary phases governs resolution in chromatographic separations. Transport in the mobile phase occurs primarily by convection, and in the stationary phase, primarily by diffusion. Differential protein adsorption essentially causes chromatographic protein separations[1]. Bead properties such as particle diameter, pore diameter, and porosity, thus influence separation efficiency because they influence the surface area to volume ratio S/V in the stationary phase. Recent innovations in chromatographic separations change S/V and the balance between convective and diffusive transport. For example, nonporous particles reduce S/V and eliminate diffusion. These media diminish both retention time and throughput. In general, separation increases with S/V, and capacity is inversely proportional to diffusion in the column. Also different particle geometries can change S/V. Cylindrical particles thus enhance throughput without sacrificing resolution, compared to spherical particles[4]. Hollow-fiber media accordingly offer enhanced mass transfer without the increased pressure drops and typical disadvantages like bed compression.

Flow-through chromatography also enhances mass transfer for a given pressure drop but without altering particle, or bed, geometry, compared to conventional media. Conventional media are typically xerogels, fragile and requiring care in handling. The d_p of a typical xerogel is on the order of 10 μm with a pore diameter d_{pore} on the order of 100 Å. Proteinaceous solutes enter the pores predominantly by diffusion. Separation is largely effected by adsorption. Smaller protein molecules exhibit greater diffusion into the pores, have more intraparticle surface area available to them for adsorption, and are retarded by the chromatographic column, thus separating them from larger proteins[31].

Particles of conventional chromatographic media are highly porous and susceptible to bed compression due to their low stiffness[12]. Bed particles move, deform, break, and are jammed into the column frit in this compression process[32]. Such chromatographic media consist of polysaccharide beads or particles, typically agarose, dextran, or cellulose, which are uncharged, hydrophilic, and as desired, fail to induce significant solute denaturation. Increasing volume, but decreasing rigidity

considerably, hydration expands xerogels. They withstand pressure drops ≤ 30 psi without substantial compression. Excessive pressure drops reduce the interstitial and pore volumes and can severely compromise throughput. Numerous strategies have been attempted to improve the separation efficiency of xerogels, with slight success. Heavily internally crosslinked xerogels are stiffer and can withstand pressure drops of 300 psi, but are too hydrophobic. These are susceptible to dead spaces, interfere with protein diffusion in the stationary phase, and fail to separate proteins effectively. Larger column diameters, rather than high pressure drops, remain preferable to process larger sample sizes. Also resolution suffers from residual protein denaturation and considerable adsorption, intrinsic to the technique. Recycling chromatography has been simulated with the equilibrium-dispersive model of chromatography. The technique displays the same limitations of prolonged retention though resolution is improved and solutes in larger samples can occasionally be resolved[33].

Analytical chromatography of protein solutions has been traditionally conducted using high-performance liquid chromatography (HPLC). HPLC media, or aerogels, consist of silica gels. These are rigid, macroreticular particles that can withstand the elevated pressure drops of the technique. Accordingly HPLC enhances resolution and decreases resolution time. However the high pressures utilized in turn demand exotic, high modulus columns and fittings. These include stainless steel columns, and suitably rigid fittings and often disfavor preparative applications. HPLC separations are also performed primarily as solute diffusion into pores followed by adsorption. Fast Protein Liquid Chromatography (FPLC©) is intermediate between HPLC and preparative protein chromatography with intermediate resolution and pressure drops.

HPLC particles are limited by flow conditions to diameters of typically 3-5 μm, with 2 μm as a lower limit below which little further speed and resolution are obtained. The small enhancements in separation obtained with smaller particle sizes also introduce prohibitively high back pressures and difficulties in column packing[34]. If porous, d_{pore} is also on the order of 100 Å. Unfortunately, often proteins coalesce around porous HPLC particles, form an impenetrable shell, and prevent diffusion into particles[1]. Increasing d_{pore} to 1000 Å, intraparticle transport can still be diffusion-limited and inadequate. Thus the diffusivity of ovalbumin, labelled with ^{19}F, in 30 μm diameter silica gel-filtration particles with such pores is diminished. Pulsed-field gradient NMR reveals that cross-sectional average diffusivity in the pores $\mathcal{D}_p$ is but about 40% of that in free solution[35]. It has been demonstrated that HPLC media also experience bed compression. At moderate packing pressures, compression reduces the interstitial porosity and enhances column efficiency for crosslinked agarose particles[32]. These results were interpreted using a relationship between column resolution and the ratio of intraparticle to interstitial porosity.

Continuous HPLC columns have also been developed. A monolithic silica xerogel[36], which possessed a d_{pore} of 2 μm, separated small organics using reversed-phase chromatography. Monolithic silica columns have been formulated that exhibit bimodal pore distributions.

The pores in flow-through particles are averred to be bimodally distributed in diameter[12,31,37]. This is often a primary characteristic of flow-through chromatography, which thus hypothetically benefit both from the high surface area of conventional media and from the high resolution of HPLC. However this is neither a

necessary nor sufficient condition for flow-through behavior which arises when there is sufficient intraparticle convection (see "Transport Theory"). In PerSeptive BioSystems media, one pore group, the diffusive pores, elicits diffusion through pores 500-1500 Å in diameter. Diffusion-limited, none of these diffusive pores is more than 10,000 Å from a throughpore. Convective transport occurs in larger "throughpores," with d_{pore} 6000-8000 Å and a length of 1000 Å. Scanning and transmission electron micrographs of various POROS media confirm these dimensions for bimodally distributed pores[12]. Excessive diffusion is prevented, but can be tailored for specific applications. Macroporosity will diminish the modulus and rigidity of larger particles less than those of smaller particles, and flow-through particles have a diameter of 10, 20, or 50 μm, ten times that of HPLC particles. By design particle diameters correspond to:

$$d_p \geq 10 \text{ throughpore diameter} \sim 100 \text{ diffusive pore diameter.} \quad (1)$$

Of course, it is more difficult to demonstrate the intraparticle convection claimed for flow-through media. Rodrigues et al. conducted experiments that implied intraparticle convection. Bovine serum albumin was accordingly chromatographed[38] on an ion-exchanger of POROS Q/M media suspended in 20 mM TrisHCl, pH 8.6. The albumin was applied to the column as a pulse and eluted with a gradient of 0.5 M NaCl. Breakthrough and elution curves were plotted as eluted protein concentration normalized with respect to feed protein concentration vs. feed mass. The curves converge for volumetric flowrates of 2, 5, and 7 ml/min, implying intraparticle convection.

It is easier to show the often exceptional permeability of flow-through particles or conditions promoting intraparticle convection (see "Transport Theory"). The two approaches can be combined to calculate the permeability of flow-through media [1, 19], which is substantially greater than that of conventional media. Pfeiffer, Chen, and Hsu measured the permeability of PSDVB flow-through media directly[39]. They determined a permeability about ten times higher than that previously determined for these media, implying intraparticle convection.

Typical flow-through media withstand highly elevated pressures. Often these media[32] experience little degeneration for pressures below 41,000 kPa. Higher pressures decrease the permeability of the chromatographic bed so that column efficiency suffers. It should be noted that flow-through media can also experience bed compression that enhances column efficiency. In particular, it has been demonstrated that packing pressures below 18,000 kPa increase the efficiency of flow-through columns by decreasing the interparticle porosity[32]. It was surmised that thus more flow is diverted through the particles increasing intraparticle convection. Polymer Labs flow-through media were used to demonstrate these relationships using urea or nitromethane as a molecular probe in a solvent of acetonitrile and trifluoroacetic acid in water. These were predicted by substituing the Carmen-Kozeny relationship into a relationship expressing the dependence of interparticle porosity on the pressure exerted on particles in the column. Pressures above 41,000 kPa fail to alter the bed porosity of Polymer Labs flow-through media[19], but compress the bed at the downstream end of the column. Suitable operating ΔP is related to the column

diameter d_{column}. In flow-through chromatography, the relationship between ΔP and v_0 is linear if for a d_{column} of 4.6 mm, $\Delta P \leq 2900$ psi (20,000 kPa) using PLRP-S 1000 or 4000 Å (Figure 2). Bed compression is averted expanding d_{column} to 2 cm if $\Delta P \leq 2000$ psi (14,000 kPa). Particles with $\Delta P \leq 5200$ kPa, or even 700 kPa, can be selected to conduct benchscale experiments inexpensively[33].

The HyperD matrix possesses some of the transport characteristics associated with flow-through media. HyperD sustains high flow rates, increasing chromatographic efficiency[25]. These media can process larger samples than typical HPLC media, and HyperD is viable for $\Delta P \leq 14{,}000$ kPa. However HyperD is compressible. The hydrogel phase in HyperD possesses high adsorption capacity for solutes, but entirely collapses when unsupported. Solutes undergo high diffusion and undetermined convection into the viscoelastic acryl-based hydrogel. High flowrates, capacity, resolution, and recovery are obtained with moderate pressure drops.

TRANSPORT THEORY

Flow-through chromatography shares a primary characteristic of membrane chromatography[8], continuous-phase chromatography, and "hydrodynamic chromatography": namely, to reduce the mass transfer resistance caused by diffusion in the pores of the chromatographic medium. Hydrodynamic chromatography uses nonporous, or pellicular, media, thus eliminating diffusion in pores. Pellicular media decrease retention time and preserve acceptable resolution. For instance, BioChrom Labs has developed nonporous PSDVB media with an enhanced, "fuzzy" surface area for these applications[40]. Biotage has developed nonporous polybutadiene-coated particles of alumina. Thus resolution can be enhanced, compared to many porous media.

Flow-through chromatography nevertheless possesses explicit advantages compared to chromatography using nonporous media, a distinction[41] made over twenty-five years ago. The mass-transfer effects between the two media were compared simulating chromatography with a continuum modelling interstices between beads and bead pores into respectively large and small pores throughout the column modelled (Figure 5). The distribution of solute molecules between the two pore types is then modelled stochastically to reveal two large advantages of flow-through chromatography: larger dynamic loading capacity and less band-broadening. Shifting the transport balance from solute diffusion to convection as found in flow-through media enhances these advantages. In a series of polymer solutes with different molecular weights, the largest solutes seldom enter bead pores. A separation mechanism results in which the larger solutes elute from the column first. These relationships are revealed examining v_0, which is given by

$$v_0 = Q/A_0 \qquad (2)$$

where Q is volumetric flowrate and A_0 is the cross-sectional area of the empty column. The height of a theoretical plate H can be nearly constant with respect to increasing v_0 at high v_0, similar[42,43] to flow-through chromatography.

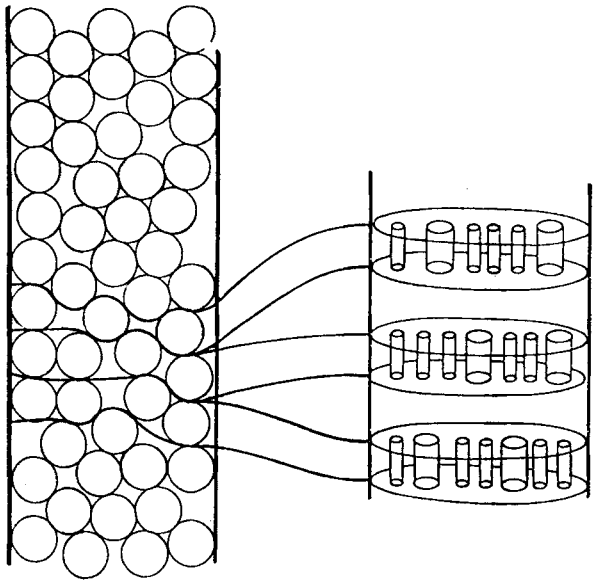

Figure 5. The bank model of a size-exclusion column. The large tubes in a given bank (on right) represent the totality of interstices at that level in the column (on left). The small tubes in this bank represent the totality of pores within the beads at this level. The space between banks serves as a mixing region and has no volume. The available volume in each bead is viewed as consisting of a labryinth of fine capillaries through which fluid can both diffuse and flow (from ref. 36). Reprinted with permission, Macromol., 3, 681 (1970). Copyright 1970, the American Chemical Society.

Models of flow-through chromatography often solve the equation of continuity for eluite mass transfer in the column. Momentum and mass transfer both occur in flow-through particles due to intraparticle convection. The apparent diffusivity $\mathcal{D}_{app}$ compared to the molecular diffusivity of the eluite $\mathcal{D}$ is enhanced. Solution reveals that in the van Deemter[11] equation,

$$H = H_{disp} + H_{int} + H_{ext} \qquad (3)$$

intraparticle convection in addition to diffusion reduces H. H_{disp} is the contribution to H due to eddy dispersion of the eluite in the chromatographic column, H_{int} is the contribution due to intra- and interparticle axial eluite molecular diffusion, H_{ext} is the contribution due to eluite mass transfer from the bulk phase to the particle surface. H_{disp} represents the influence of column backflow on eluite transport and equals a constant, typically 1 at appreciable flowrates[8]. The interstitial velocity v_b differs from v_0:

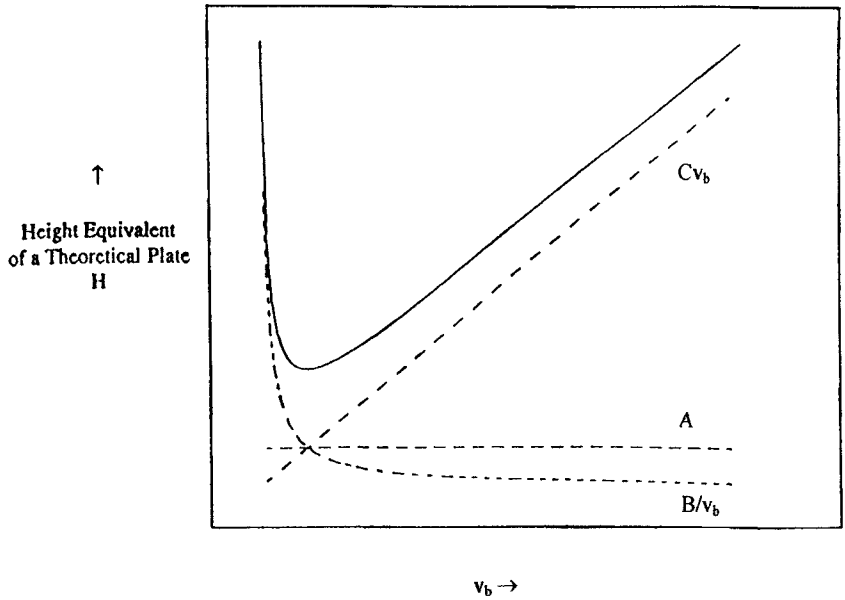

Figure 6. An illustration of the contributions to H vs. v_b. Reprinted with permission, Sep. Purif. Meth., 25, 47 (1996). Copyright 1996, Marcel Dekker, Inc.

$$v_b = L/\tau_r \tag{4}$$

where L is longitudinal bed length and τ_r is the retention time of a molecular probe completely excluded from the chromatographic medium. The difference is observed in the interparticulate porosity ε_b:

$$\varepsilon_b = v_0/v_b \tag{5}$$

H_{int} and H_{ext} depend on v_b so that H does[11] (Figure 6). Typically

$$H_{int} = B/v_b \tag{6}$$

where B is[8] often 0.8. Excellent reviews are available discussing the physical significances of H_{disp}, B, and other constants in the H_i expressions[8,44].

Expressions for flow-through H vary, primarily in the form of H_{ext}. H for conventional and flow-through packings is compared in Figure 3. Figure 6 illustrates that eliminating H_{ext} would decrease H. Pellicular packings accordingly display the advantages of lower H. Experiments with nonporous packings show that H fails to

eliminate the v_b dependence of H_{ext} entirely, but conforms to the Knox equation, a variation on equation (3):

$$h = Av^{1/3} + B/v + Cv \tag{7}$$

H_{disp} for the Knox equation depends on v and hence v_b taken to the one-third power. Accordingly h depends on v at low to intermediate v, as shown in Figure 7. $H(v_b)$ can be expressed in dimensionless form as $h(v)$, where h is the reduced plate height:

$$h = H/d_p \tag{8}$$

and v is the reduced eluite velocity:

$$v = v_b d_p/\mathcal{D} \tag{9}$$

For flow-through packings, H_{ext} is also velocity-dependent. Decreasing d_p also decreases H_{ext}. Models of flow-through chromatography show H is decreased because intraparticle convection dramatically decreases H_{int}, which is proportional to v_b^{-1} Moreover H_{ext} has a form in which H_{ext} decreases with d_p. Ordinarily H_{ext} also depends on particle geometry and mode of mass transfer[11]:

$$H_{ext} = C(\text{geometry})v_b \tag{10}$$

C(geometry) depends on the bed and particle porosities, respectively ε_b and ε_p, as well as the adsorption equilibrium parameter b for a linear isotherm with slope m:

$$C(geometry) = \frac{2}{3}\left\{\varepsilon_p(1-\varepsilon_b)b_2/\left[\varepsilon_b + \varepsilon_p(1-\varepsilon_b)\right]_2\right\}\tau_d v_b \tag{11}$$

where ε_p is the intraparticulate void fraction and ε_b the interparticulate void fraction. In equation (11), these results can easily be generalized to spherical particles by replacing 2/3 with 2/15. τ_d is the time constant for intraparticle diffusion and for a slab ℓ thick, is expressed:

$$\tau_d = \varepsilon_p \ell^2/\mathcal{D}''_e \tag{12}$$

using $\mathcal{D}''_e$ as the eluite diffusivity in diffusive pores.

Different assumptions and solution techniques can be applied to solve the equation of continuity for the eluite for flow-through chromatography. The model of Rodrigues et al. [11,45,46] developed equations (10) and (11), which assume film mass transfer for solute transport from the bulk phase to the surface of chromatographic particles. The model includes a linear adsorption isotherm exhibiting finite sorption kinetics, simulating Langmuir behavior at low solute c_b. Accordingly the influences of

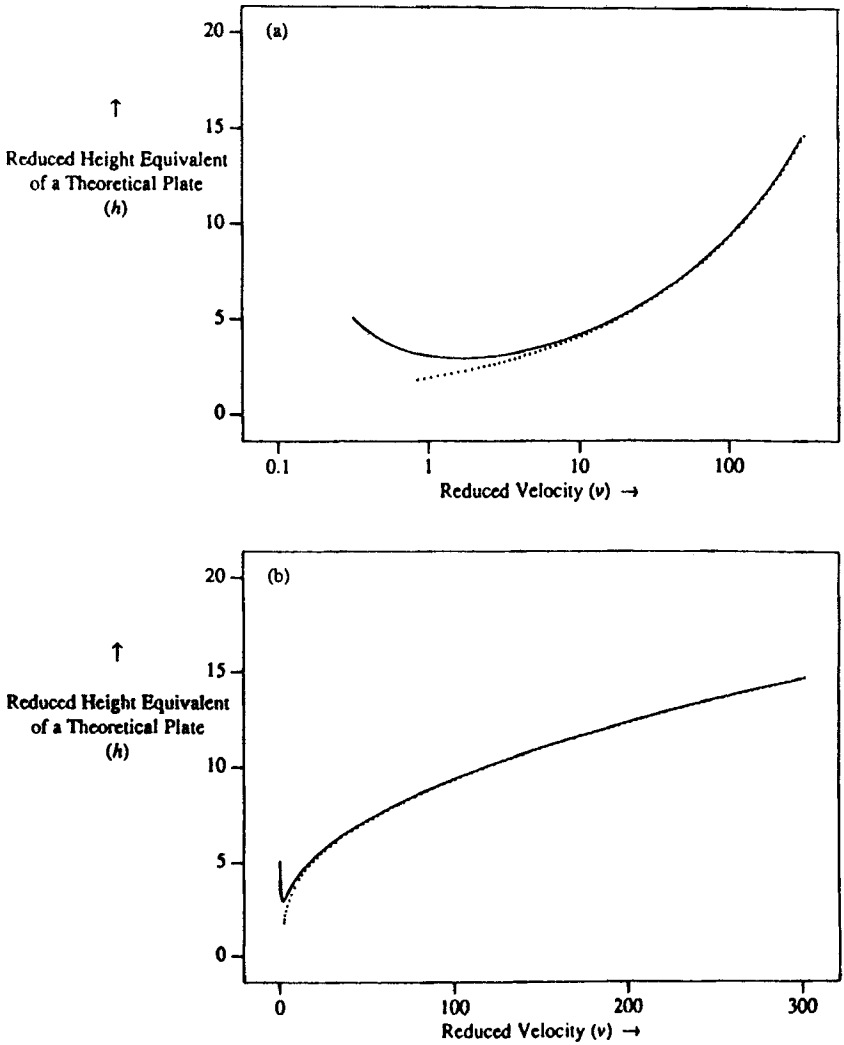

Figure 7. The dependence h on v for the Knox equation with (a) plotting v on a logarithmic scale and (b) on a linear scale. At high v, h becomes constant. Reprinted with permission, Sep. Purif. Meth., 25, 47 (1996). Copyright 1996, Marcel Dekker, Inc.

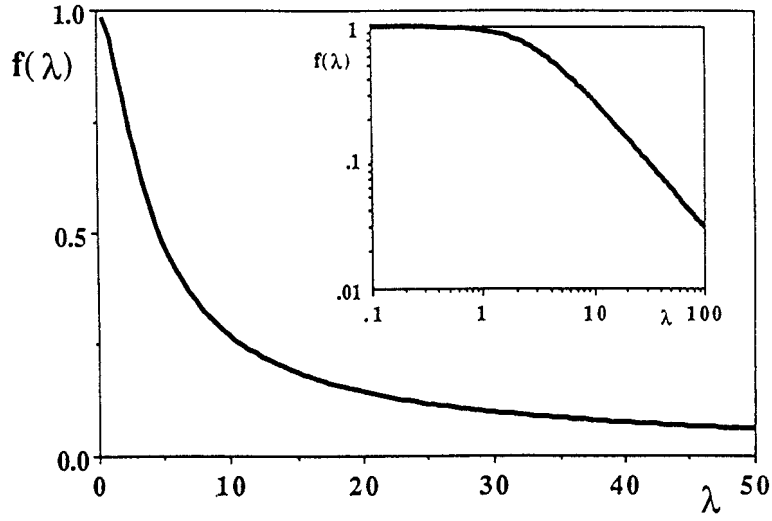

Figure 8. Linear and (inset) logarithmic plots of f(λ). Reprinted from Chem. Eng. Sci., 46, 2765, copyright 1991, with permission from Elsevier Science Ltd., The Boulevard, Langford Lane, Kidlington OX5 1GB, UK.

diffusion and sorption on flow-through separation can be compared. The model was developed for large-pore particles with a slab geometry. Without considering eluite sorption kinetics, Rodriques derived a modified van Deemter equation for slab-like particles,

$$H = H_{disp} + H_{int} + C(\text{geometry})f(\lambda)v_b \quad (13)$$

In equation (13), f(λ), as shown[46] in Figure 8, represents the relative predominance between diffusive or convective intraparticle transport. λ is[11] the intraparticle Pèclet number, at a given v_b' and ℓ, the half-thickness of slab particle:

$$\lambda = v_b'\ell/\mathcal{D}''_e \quad (14)$$

v_b' is the intraparticle superficial velocity. f(λ) relates the permeability, tortuosity, particle diameters (flow-through >> subsidiary), and effective eluite diffusivity of the diffusive pores to those of the throughpores:

$$f(\lambda) = 3/\lambda(1/\tanh\lambda - 1/\lambda) \quad (15)$$

f(λ) also depicts eluite adsorption and contains the eluite equilibrium constant between the bulk and adsorbed phases. If diffusion predominates, $\lambda \rightarrow 0$ and $f(\lambda) \rightarrow 1$. If

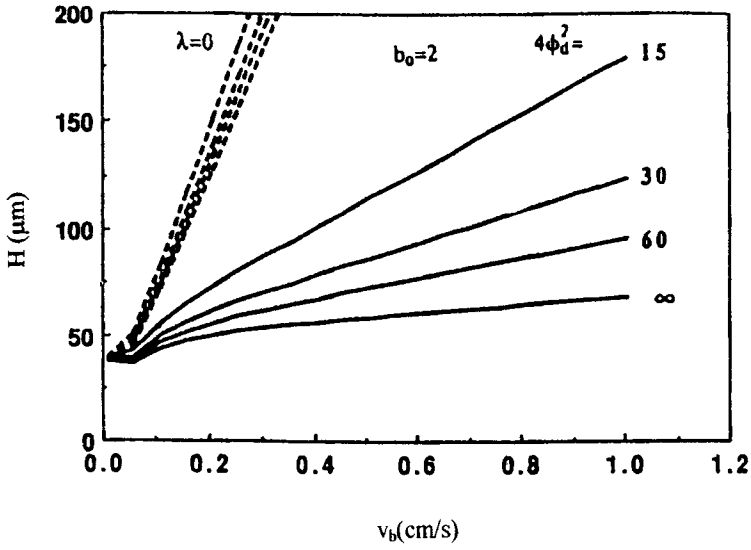

Figure 9. The dependence of H on v_b for adsorption/desorption. Separations using intraparticle convection depend on ϕ_d. Conventional media = – – –; flow-through media = ——— Reprinted from Chem. Eng. Sci., 47, 4405, copyright 1992, with permission from Elsevier Science Ltd., The Boulevard, Langford Lane, Kidlington OX5 1GB, UK.

convection predominates, λ becomes large and $f(\lambda) \rightarrow 3/\lambda$. At high v_b, the term for H_{ext} in equation (13) behaves so that H becomes nearly constant. Rodrigues adapts his model to spherical particles as indicated above[11]. His model can also depict adsorption kinetics, whether slow or infinitely fast. For adsorption, H_{ext} contains additional terms depicting film mass transfer and the rate-limiting step for mass transfer:

$$H_{ext} = C(\text{geometry})\,[f(\lambda) + 3/Bi_m + 3(b - 1)/b^2\phi_d^2]v_b \qquad (16)$$

where Bi_m is the Biot number, accounting for film mass transfer

$$Bi_m = k_f d_p / \mathcal{D}''_e \qquad (17)$$

and ϕ_d is the Thiele modulus, based upon desorption

$$\phi_d = \tau_d k_d \qquad (18)$$

The film mass-transfer coefficient is k_f and the desorption rate constant k_d. Figure 9 shows the influence of ϕ_d on H for conventional and flow-through media. For flow-

through media, an increase in ϕ_d decreases the dependence of H on v_b. Rodrigues originally used many of the concepts above to depict the transport in catalyst particles with exceptionally large pores[11]. Such studies illuminate study of flow-through chromatography as will be seen below[47].

Using the Blaze-Kozeny equation for momentum transport in a packed bed, Afeyan et al.[1] demonstrate that the pore velocity v_{pore} can display appreciable intraparticle convection and reach 5% of v_0. This justifies claims that flowthrough configurations increase v_{pore} and separation efficiency dramatically. A v_{pore} that is 1% v_0 suffices to increase the particle Péclet number Pé to 10 or more so that flow-through effects are manifested[28]. The Blaze-Kozeny equation relates the bed permeability K to its void fraction ε_b:

$$K = \varepsilon_b^3/150(1-\varepsilon_b)^2 \tag{19}$$

K is also related to d_p, v_0, and the mobile phase viscosity μ:

$$K = \mu v_0/d_p^2(\Delta P/L) \tag{20}$$

Rearranged, equation (20) furnishes an expression for v_0. Analogous relationships depict fluid flow in the throughpores so that

$$v_0/v_{pore} = K_p d_m^2(1-\varepsilon_b)/K d_p^2\,\varepsilon_p \tag{21}$$

where K_p is the particle permeability and depends on ε_p. Using a large v_0 of 1000 cm/h, conventional estimates of the diameters, permeabilities, and porosities in equation (21) predict a v_{pore} of 50 cm/h for a 7000 Å pore diameter and a 10 μm d_p. This v_{pore} is similar to the v_0 typical of soft gel media. The flow-through regime of mass transport occurs when Pé >> 1:

$$Pé = d_p v_0/2\mathcal{D} \tag{22}$$

Pé represents the ratio of mass transport by convection to that by diffusion. Pé >> 1 means convection dominates mass transport across the particle, which can be taken to signify nonneglible intraparticle convection. The model shows that the apparent pore diffusivity $\mathcal{D}_{app}$ is proportional to the bed velocity for flow-through behavior:

$$\mathcal{D}_{app} = \mathcal{D} + d_p v_0/2 \cong d_p v_0/2 \sim v_0 \tag{23}$$

For a 7000 Å pore diameter and a 10 μm d_p, the Pé is 57 and flow-through enhancement of intraparticle mass transport occurs. This model provides a convenient relationship between particle characteristics and the likelihood that intraparticle convection will occur. However it has been claimed that calculations for intraparticle convection based on the Blaze-Kozeny equation overestimate the effect of intraparticle

Pé. This model, called the Frey-Scheinheim-Horvath or FSH model, predicts for H:

$$H = 1/(1/H_{disp} + 1/Ev_0) + B/v_0 + F \quad (24)$$

where E and F are empirical constants with different significances than the aforementioned H_{disp}, B, and C.

The model of Frey *et al.* uses assumptions, perhaps closer to actual eluite transport in chromatography[44]. Many relationships for h(Pé) in this model resemble those in the Rodrigues model. For instance, the Frey *et al.* model assumes a linear mass transfer driving force proportional to the difference between the eluite concentration in the bulk phase and as an average, in the throughpores. Adsorption is assumed instantaneous and fits a linear isotherm. Each flow-through particle (denoted by a prime) is divided into "subsidiary particles," (denoted by double prime), between which intraparticle convection occurs. For example, the effective diffusivity of the eluite in a throughpore is $\mathcal{D}'_e$ and in a diffusive pore is again $\mathcal{D}''_e$; both are proportional to $\mathcal{D}$. Consequently "hindered diffusion" is depicted within a flow-through particle. Slab and spherical geometries are considered, as well as diffusive transport of the eluite. For a spherical geometry, the apparent effective intraparticle diffusivity of the eluite $\mathcal{D}_{app}$

$$\mathcal{D}_{app} = g(1 + 2P\,Pé'/45)\mathcal{D}'_e \quad (25)$$

predicts a dependence on f and the throughpore Péclet number Pé':

$$Pé' = v_{pore}/d_p\mathcal{D}'_e \quad (26)$$

$\mathcal{D}'_e$ depends on the intraparticle tortuosity θ' and intraparticle hindrance parameter χ':

$$\mathcal{D}'_e = \mathcal{D}\chi'/\theta' \quad (27)$$

Equation (25) replaces the 1/2 in the approach of Afeyan *et al.* in equation (23) with 2/45. The dependence of $\mathcal{D}_{app}$ on Pé' in equation (25) is significantly lower than the preceding models described. For a slab geometry, the apparent intraparticle diffusivity of the eluite $\mathcal{D}_{app}$

$$\mathcal{D}_{app} = g(1 + Pé'/6)\mathcal{D}'_e \quad (28)$$

predicts similar dependences. The Rodriques model has a f(λ) that differs from g in form

$$g = \left[1 + \frac{(1-\varepsilon')\varepsilon''^2(1+K_{eq})^2}{(\varepsilon' + (1-\varepsilon'')\varepsilon'(1+K_{eq}))}\frac{D_e'\varepsilon'}{D_e''\varepsilon''}\left(\frac{d_p''}{d_p''}\right)^2\right]^{-1} \quad (29)$$

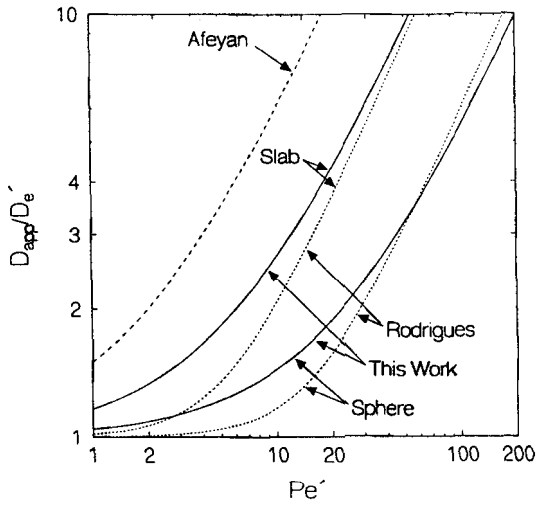

Figure 10. Normalized apparent intraparticle diffusivity vs. Pè' for a different models of intraparticle convection. Reprinted with permission, Biotech. Prog., 39, 273 (1993). Copyright 1993, the American Chemical Society, Inc.

though the physical meanings are similar. The volume fraction of gigapores is ε' and the diameter of a subsidiary particle d_p'' in the notation in equation (29). For an eluite distributed between the mobile and stationary phases, K_{eq} is the Henry's law equilibrium constant. Figure 10 illustrates the dependence of $\mathcal{D}_{app}/\mathcal{D}'_e$ on Pé' for the Frey *et al.* model compared to those of Afeyan *et al.* or Rodriques. For various ratios of flow-through and subsidiary particle diameters, the Frey *et al.* model illustrates that intraparticle convection significantly diminishes h as a function of Pé. The model fits experiments well for separations of numerous proteins in a gel-filtration mode, debatable for flow-through chromatography. Moreover data collected for a number of pore diameters demonstrated that resolution strongly depends on available surface area for adsorption, as expected. The model demonstrated that the resolution obtained in short elution times was even greater for nonporous, pellicular media than for the flow-through media evaluated, in contrast to a stochastic model[41] and others. This superiority is shown in Figure 11, illustrating h vs. Pé. Moreover this approach exhibited fine conformity for the flow-through chromatography of small proteins using commercial packings (Figure 12). The smaller the protein, the better the model fits as shown in Figure 13, which gives plate height in tryptophan chromatography. The assumption of a linear driving force for mass transfer has been claimed to be inappropriate to depict intraparticle convection. Any inadequacies in the Frey model would perhaps be induced by this assumption.

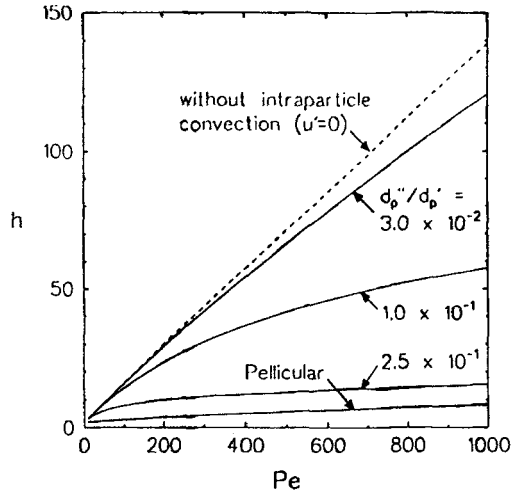

Figure 11. A comparison of h vs. Pe for various column packings, but with dimensionless retention time k' of 2. Furthermore $\theta' = 4$, $\chi' = 1$, and $\varepsilon' = 0.4$. Reprinted with permission, Biotech. Prog., 39, 273 (1993). Copyright 1993, the American Chemical Society, Inc.

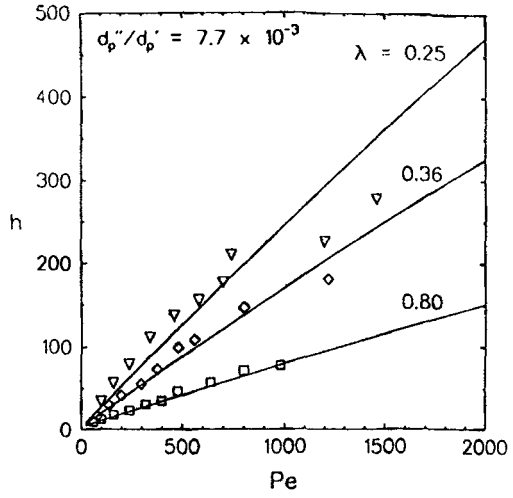

Figure 12. Reduced plate height as a function of Pè for a ratio of subsidiary particle diameter to particle diameter of 7.7 x 10^{-3}. Theoretical lines were calculated for no intraparticle convection, but with A = 2.5, B = 1.6, $\theta = 8$, $\alpha = \varepsilon = 0.4$, k' = 0, and various values of l as indicated. Experimental data were obtained on Polymer Labs PLRP 300 Å media for lysozyme (□), carbonic anhydrase (◊), and amylase (▽) under conditions of no retention. Reprinted with permission, Biotech. Prog., 39, 273 (1993). Copyright 1993, the American Chemical Society, Inc.

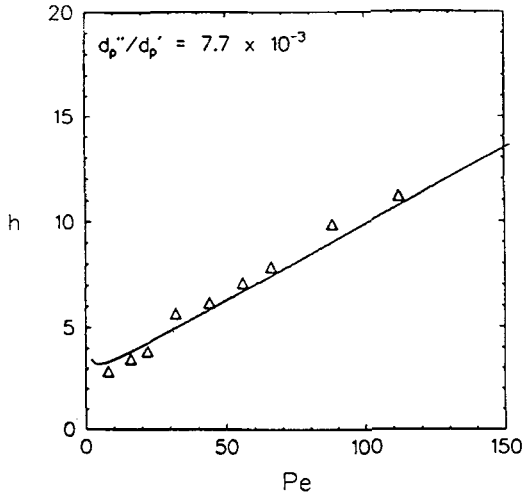

Figure 13. Reduced plate height as a function of Pè for a ratio of subsidiary particle diameter to particle diameter of 7.7×10^{-3}. Theoretical lines were calculated for no intraparticle convection, but with A = 2.5, B = 1.6, $\theta = 8$, $\alpha = \varepsilon = 0.4$, k' = 0, and u' = 0. Experimental data were obtained on Polymer Labs PLRP 300 Å media for tryptophan under conditions of no retention. Reprinted with permission, Biotech. Prog., 39, 273 (1993). Copyright 1993, the American Chemical Society, Inc.

Other models of flow-through chromatography emphasize transport contributions and effects. For instance, the Frey et al. model qualitatively predicts enhanced frontal analysis for flow-through chromatography, similar to the predictions obtained from the model of Liapis and McCoy[48]. The latter model analyzes the effect of intraparticle convection on the percent adsorptivity as a function of time and breakthrough rather than analyze the effect on H. Thus the column feed need not simulate the Dirac delta function used by other models[49] and resembles real chromatographic systems more closely. A number of additional assumptions different from the other models are used. For instance, nonlinear adsorption is assumed, according to the Langmuir isotherm. Slow, relatively fast, and infinitely fast adsorption rates are analyzed as well as multieluite solutions. The remaining models in the literature often assume infinitely fast adsorption rates and fail to depict numerous real chromatographic systems. Furthermore these models are often restricted to use of a linear adsorption isotherm. Liapis and McCoy confined their analysis to the intraparticle mas transfer resistances. They had shown earlier that for purely diffusive particles extraparticle mass transfer resistance was negligible compared to the intraparticle mass transfer resistance[50]. A slab geometry is assumed. Orthogonal collocation is used to solve for the eluite bulk, pore, and surface concentration profiles numerically. As expected, intraparticle

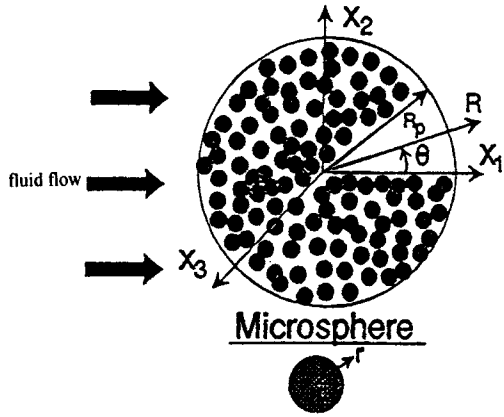

Figure 14. Spherical perfusive adsorbent particle with a bidisperse porous structure. R_p = radius of a perfusive particle, r_m = radius of a microsphere. Reprinted with permission, J. Chromat. A, 704, 45 (1995). Copyright 1995, Elsevier Publ.

convection increases the eluite pore concentration, in turn, increasing the eluite surface concentration. Flow-through increases the percent adsorptivity as a function of percent breakthrough or time, particularly at short times. The respective antibodies of lysozyme and β-galactosidase were immobilized on affinity columns and used to confirm this model. This provides well-characterized, exemplary affinity media to examine the characteristics of flow-through chromatography and fits the data well.

Liapis and his colleagues recently applied orthogonal collocation to depict flow-through in spherical particles[51,52]. These consist of microparticles in which only diffusion occurs (Figure 14) as they do for the Frey et al. model. Intraparticle convection occurs between microparticles, the location of throughpores. Thus there are three transport regimes: bulk liquid, throughpores, and diffusive pores. Concentration profiles are provided in each of these for simple Langmuir kinetics[51]. Flow-through particles with a d_p 15 μm and the eluite, bovine serum albumin, were used for these simulations. The mechanisms of external film mass transport around the adsorbent particles and of axial dispersion on the column were considered to have negligible contributions to the overall mass transprt resistance for reasons given in the literature. Of particular interest are the eluite concentration C_p and average adsorbed concentration C_{sa}. For convenience, C_p is normalized with respect to the eluite concentration in the bulk phase $C_{d,in}$ and C_{sa} is normalized with respect to the eluite concentration indicative of maximum adsorption capacity C_T as shown in Figure 15 with respective intraparticle Pé of 2, 10, and 50. As Pé' is increased, the profiles for dimensionless C_p and C_{sa} display an asymmetry displacing concentration streamlines toward the downstream half of the spherical particles. The asymmetry signifies that as intraparticle Pé is increased, more of the total adsorption capacity of the particles is

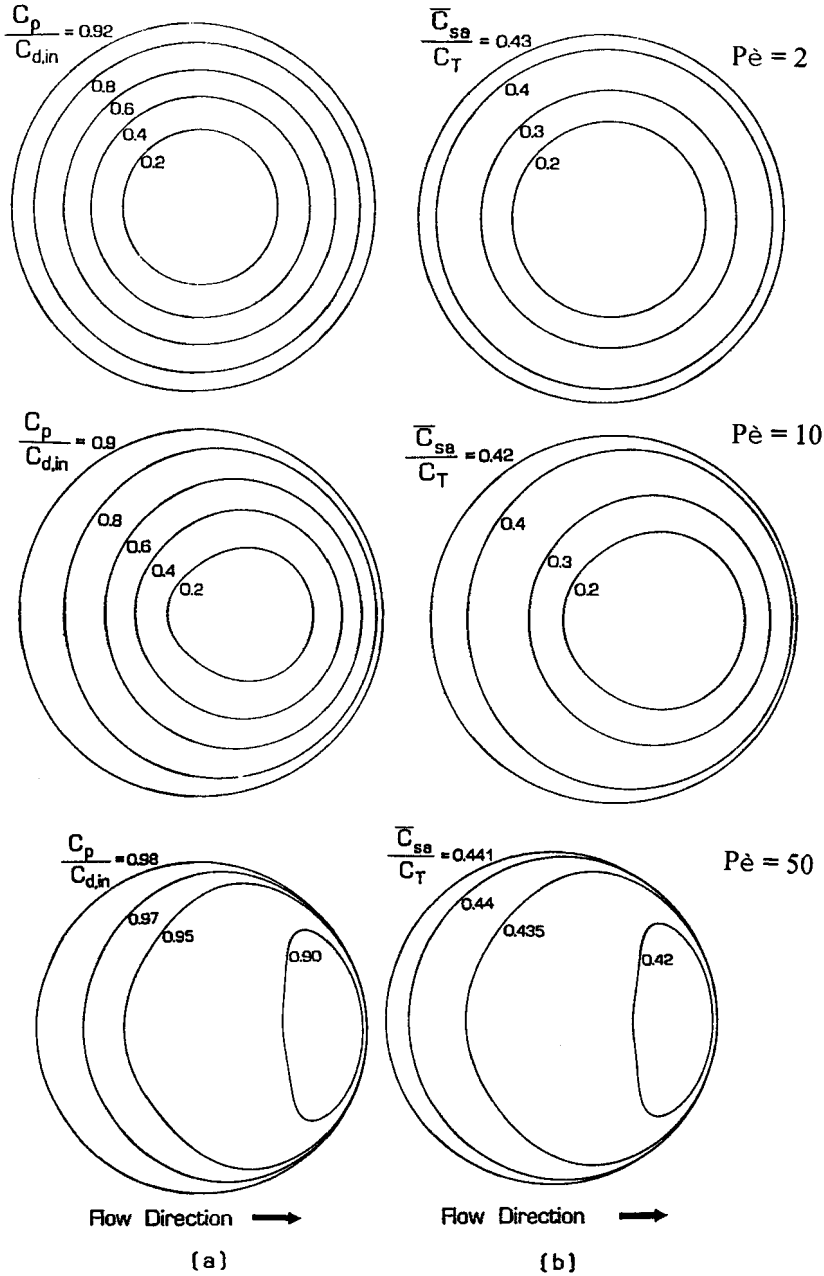

Figure 15. Isoconcentration contours of the concentration of the adsorbate in the pore fluid of the macroporous region and in the adsorbed phase of the porous adsorbent particle when $d_m = 7.13 \times 10^{-8}$ at x = 0.125L and t = 60 min. (a) $C_p/C_{d,in}$, (b) C_{ss}/C_T for Pè = 2, 10, or 50. Reprinted with permission, J. Chromat. A, 704, 45 (1995). Copyright 1995, Elsevier Publ.

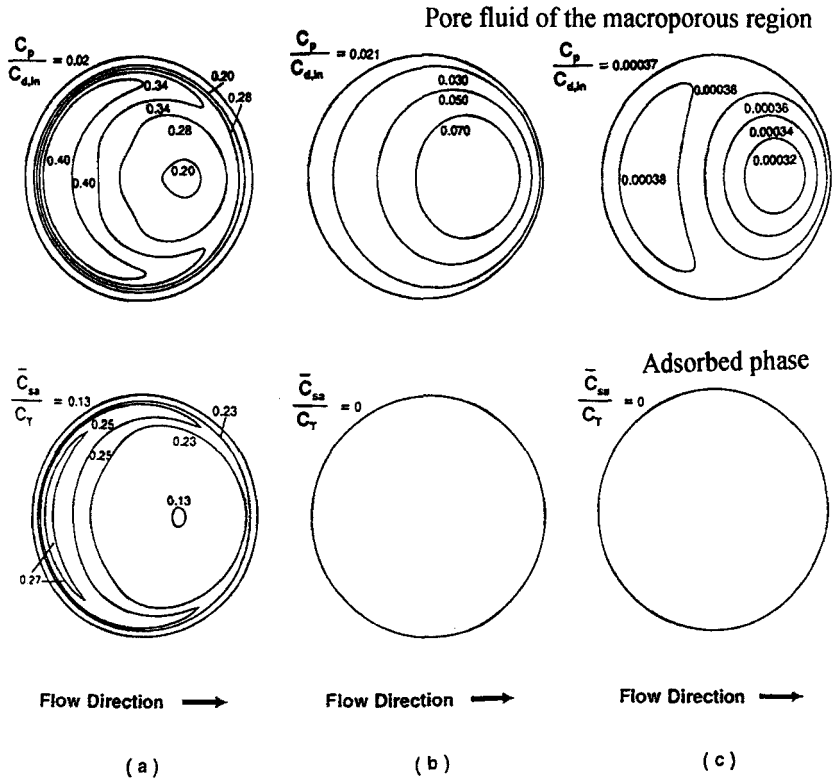

Figure 16. Isoconcentration contours of the concentration of the adsorbate in the pore fluid of the macroporous region and in the adsorbed phase of the porous adsorbent particle when $d_m = 7.00 \times 10^{-7}$ at x = 0.2L and t = (a) 0.1, (b) 0.3, and (c) 0.4 min for eluent flow countercurrent to adsorbate flow. Pè = 10 for the adsorbent, but 0.476 for the eluent. Reprinted with permission, J. Chromat. A, 724, 13 (1996). Copyright 1996, Elsevier Publ.

utilized, improving separation. More of this capacity is also utilized, decreasing particle diameter or increasing d_{pore}. Potential separation advantages emerge if the eluent is applied to the downstream end of a flow-through column[53], a configuration inverse to displacement chromatography. For given values of transport properties, isoconcentration contours for dimensionless C_p and C_{sa} were compared. The contours are highly skewed to the downstream end of the column in the inverted configuration (Figure 16), but display symmetry when both adsorbate and eluent are applied to the same end of the column. Again asymmetry indicates improved separation, due to anistropic distribution of eluite in the particles. The macropore distribution depends on eluite transport properties[54], as shown in Figure 17, where flow-through separation

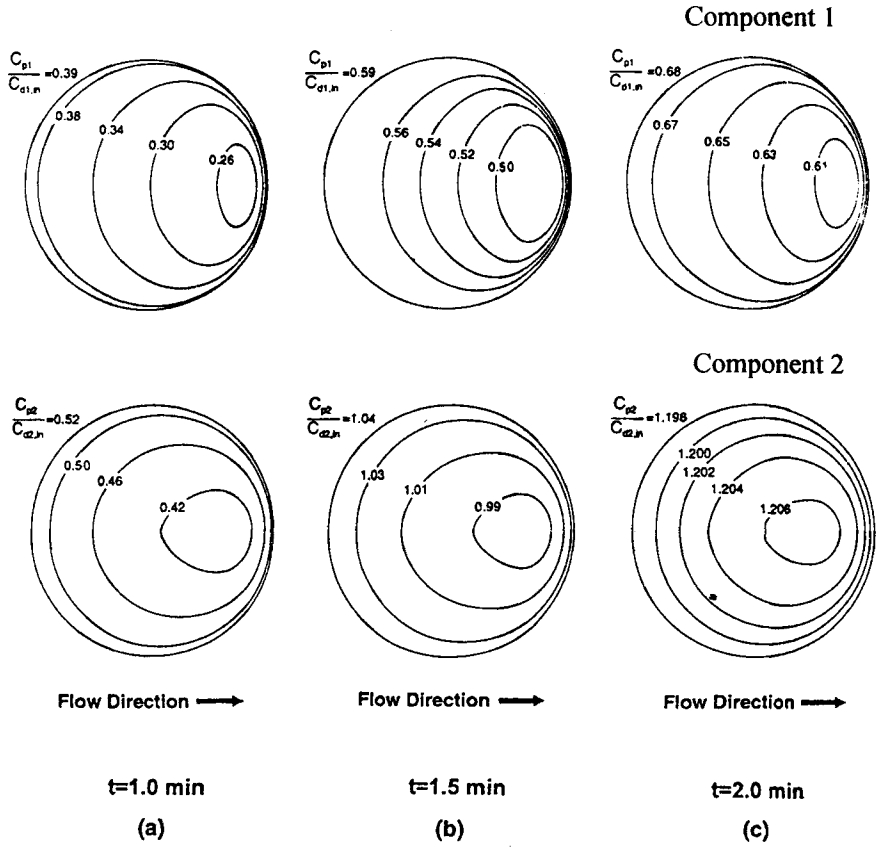

Figure 17. Isoconcentration contours of the concentration of components 1 or 2 in the pore fluid of the macroporous region of the porous adsorbent particle for v_0 = 1000 cm/h at different times and x = 0.25L. Throughpore void fraction is 0.45, d_p is 1.4 x 10^{-5} m. Equilibrium adsorbed concentrations of 1 and 2 are respectively 2.186 and 8.892 x 10^{-3}. Reprinted with permission, J. Chromat. A, 734, 105 (1996). Copyright 1996, Elsevier Publ.

of two components is simulated. The effective pore diffusivity for component 1 is nearly one-third of that of component 2; the equilibrium constant for the adsorption of component 1 to the particle surface is nearly 250 times that for component 2. Figure 18 shows that the anisotropic distribution of the different components in the macropores is amplified as eluites enter the diffusive pores and adsorb. Revealed are excellent separation characteristics.

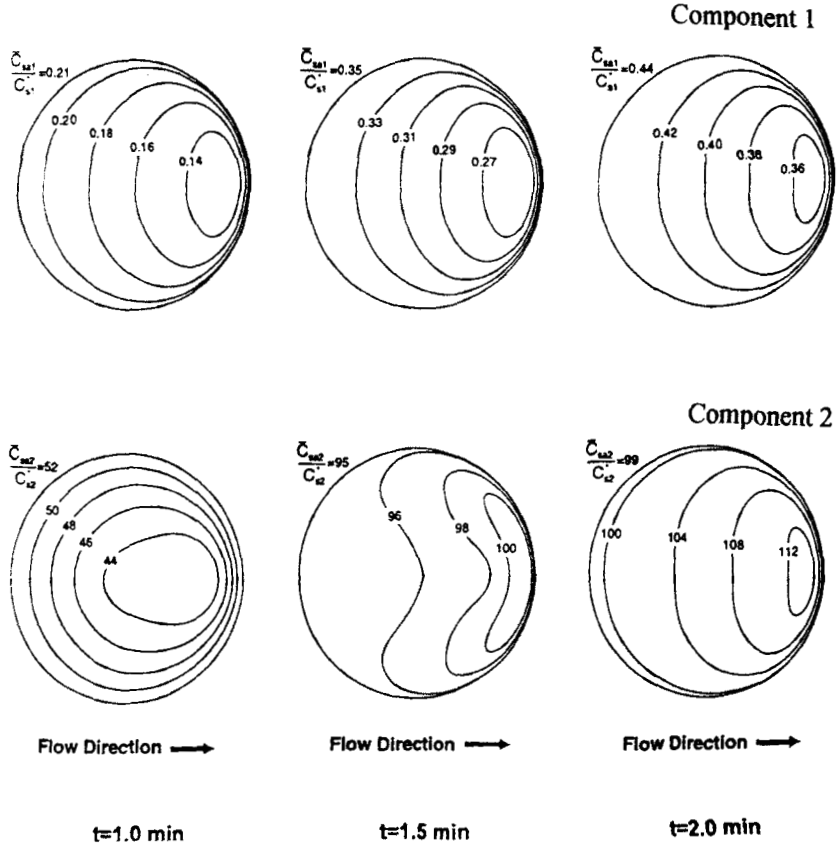

Figure 18. Isoconcentration contours of the concentration of components 1 or 2 in the adsorbed phase of the porous adsorbent particle for v_0 = 1000 cm/h at different times and x = 0.25L. Throughpore void fraction is 0.45, d_p is 1.4 x 10^{-5} m. Equilibrium adsorbed concentrations of 1 and 2 are respectively 2.186 and 8.892 x 10^{-3}. Reprinted with permission, J. Chromat. A, 734, 105 (1996). Copyright 1996, Elsevier Publ.

Liapis extended his analyses of particle characteristics. For example, he and Heeter compared separation characteristics of spherical particles which were either perfusive or purely diffusive[21]. The criteria used to compare the performance of the two media were the breakthough time, the mass of adsorbate in the adsorbed phase at breakthrough, and the percentage utilization of the adsorptive capacity of the column. A Langmuir adsorption isotherm was again used in extending his numerical simulation

of anion exchange chromatography under perfusive or purely diffusive conditions. The parameter F is the amount of column convection diverted through particles:

$$F = B/\beta^3 - 10\eta^5 A/\beta^5 \tag{30}$$

where

$$\beta = r_p/K_p^{1/2} \tag{31}$$

$$\eta = (1-\varepsilon_b)^{1/3} \tag{32}$$

$$B = 1/J[3\beta^3 + 2\beta^3\eta^5 + 30\beta\eta^5 - \tanh\beta/\beta(3\beta^3 + 12\beta^3\eta^5 + 30\beta\eta^5)] \tag{33}$$

$$A = 1/J[6\beta^3 + \beta^5 - \tanh\beta/\beta(6\beta^3 + 3\beta^5)] \tag{34}$$

$$J = 2\beta^2 - 3\beta^2\eta + 3\beta^2\eta^5 - 2\beta^2\eta^6 + 90\eta^5/\beta^2 + 42\eta^5 - 30\eta^6 + 3 - \tanh\beta/\beta(-3\beta^2\eta + 15\beta^2\eta^5 - 12\beta^2\eta^6 + 90\eta^5/\beta^2 + 72\eta^5 - 30\eta^6 + 3) \tag{35}$$

The intraparticle radial coordinate is r_p. The radial and tangential components of the intraparticle velocity are approximately proportional to v_0 and F. Accordingly, $F \geq 0$ and for intraparticle convection, F equals zero. F depends on ε_b, ε_p, ϕ, and the microparticle diameter d_m. Performance given no intraparticle convection was enhanced by decreasing d_p, increasing ε_p, and to a lesser degree, decreasing d_m. Increases in the adsorption rate constant enhance separation when this constant is relatively small.

For flow-through chromatography, performance was again enhanced decreasing d_p and increasing ε_p, but required an increase in d_m. Furthermore a decrease in ϕ enhanced performance. Equal to 150 in equation (19), which depicts bed permeability, the parameter ϕ determines the macropore permeability

$$K_p = \varepsilon_p^3/\phi(1-\varepsilon_p)^2 \tag{36}$$

but here ε_p refers to the intraparticle porosity of the macropores in equation (36). Low ϕ's correspond to higher pore connectivity in the particles due to processing. Experiment supports these results. For example, the permeability measured for PSDVB flow-through particles[39] is significantly greater than conventional media or previous prediction. Presumably low ϕ would correspond to increased intraparticle convection.

This result is supported by a previous study[47]. Therein Stephanopoulos and Tsiveriotis demonstrated that flow-through characteristics enhance separation dependent on an intraparticle Péclet number proportional to K. Their study simulated biological catalysis using a zero-order nutrient uptake rate. A regular perturbation method was incorporated to depict the flow field inside a porous spherical particle subject to external free fluid flow conditions. The model was solved analytically. It

was determined that intraparticle flow fails to influence extraparticle transport. Flow-through characteristics enhance biocatalysis by inducing anisotropy in the intraparticle concentration of nutrients in a manner similar to Figures 15 and 16. Regarding mass-transport, the results of Liapis[21] supplement this study and determine that the separation advantage of flow-through to purely diffusive media depends on d_m. There is no advantage of flow-through compared to purely diffusive media when d_m is 700 Å, but a definite advantage emerges for $d_m \geq 7000$ Å.

Heeter and Liapis extended their modelling to compare flow-through and purely diffusive particles[55]. Monodisperse pore distributions were compared to bidisperse distributions in the modelled particles. A linear adsorption isotherm was selected so that Laplace transforms solved the equation of continuity analytically for the adsorbate concentration in three transport regimes. These regimes depicted the bulk liquid, diffusive pores, and in the case of bimodal pore distributions, throughpores. Expressions for the Laplace transforms of the adsorbate concentration nonetheless could not be inverted. Accordingly expressions of the adsorbate concentrations were simulated numerically using the LSODES component of the ODEPACK software package. Experimental breakthrough behavior was simulated and compared to the model. The many parameters of the model provided the best fit when given the most plausible values.

Further investigations by Heeter and Liapis show that SOURCE media are probably purely diffusive media[22]. To do so, the breakthrough characteristics of bovine serum albumin (BSA) chromatographed on SOURCE anion exchange media were compared to dynamic adsorption models of the process. The models used either linear or Langmuir adsorption isotherms. Furthermore the SOURCE particles were assumed to contain monodisperse pores. Numerical techniques were used to simulate breakthrough curves in this model when adsorption conformed to the Langmuir isotherm, but Laplace transforms were used for simulation when adsorption was linear. The Langmuir isotherm superbly fit the data for the adsorption of BSA to the SOURCE anion exchange media. For a number of prospective breakthrough conditions, the dynamic Langmuir adsorption model fit the experimental data well. Moreover this model fit the data best when $\mathcal{D}_p$ was less than the free diffusivity of BSA in solution, circumstances that are plausible because diffusion is expected to be restricted in porous particles. There was little difference in fit for flow-through as compared to purely diffusive particles, implying that the particles need not exhibit flow-through behavior to possess good separation characteristics. In contrast, the dynamic linear adsorption model was somewhat less plausible. It fit the data well when the adsorbate concentration at the column inlet $C_{d,in}$ was 0.03 and 0.05 kg/m^3. However, when $C_{d,in}$ was 0.01 kg/m^3, this model fit the data best when $\mathcal{D}_p$ exceeded the free diffusivity of BSA, which is unlikely. In summary, Liapis's efforts demonstrate that purely diffusive particles can provide superior performance to flow-through particles if the diffusive particles possess high pore connectivity, surface area, and active sites per unit surface area as mentioned in "PSDVB Flow-Through Chemistry".

TABLE II: SPLIT RATIOS FOR 0-5000 CM/H (recast from ref. 57)

MEDIUM	$\mathcal{D}_p \times 10^{-11}$ (m^2/s)	$\alpha \times 100$
POROS 20 R1	8.9	0.71
POROS 20 R2	5.2	0.19
Oligo R3	4.2	0
POROS 50 R1	5.4	0.34
POROS 50 R2	5.4	0.11

PROTEIN SEPARATIONS

Flow-through chromatography possesses highly desireable separation properties empirically. For example, bandspreading is diminished with increasing amounts of flow diverted to the throughpores[56]. So is the percent breakthrough capacity. An increase in the "split ratio" α, the ratio of the amount of feed entering throughpores to that entering diffusive pores, decreases the sensitivity of bandwidth to flowrate. For PerSeptive BioSystem's Oligo R3, d_{pore} averages 500 Å, maximizing particle surface area. Table II shows that the split ratio falls to zero for this medium[57] unlike typical reversed-phase flow-through media such as POROS. The effective pore diffusivity $\mathcal{D}_p$ averages $\mathcal{D}'_e$ and $\mathcal{D}''_e$ and was determined along with α using nonlinear regression to fit data for the chromatography of three proteins. Implicitly intraparticle convection needs large pores or a bimodal pore distribution. At zero split ratio, bandspreading increases linearly with flowrate, but at increased split ratios, bandspreading becomes constant at higher flowrates. Protein diffusivities are typically of the order 10^{-11} m^2/s, the same order of magnitude as those calculated in Table II. Diffusion into the particle will be hindered as reflected in diminished $\mathcal{D}_p$; little hindrance is implied by Table II and is perhaps unlikely. It would also be preferable to determine split ratios directly with tracer experiments.

An increase in diffusive pore size increases flow-through, augmenting trends based on Table II. Resolution, bandwidth or dynamic loading capacity do not deteriorate for v_b of $10\text{-}10^2$ cm/h in HPLC or preparative chromatography, but do not deteriorate in flow-through columns until v_b is nearly 10^4 cm/h. The characteristics of flow-through applications fail to deteriorate and attest to the strong coupling between solute mass transport and v_b. Frontal analysis shows that breakthrough curves are not dependent on v_b for flow-through chromatography. Its dynamic loading capacity for bovine serum albumin decreases with increasing v_b, but much less steeply than for preparative media (Figure 19).

Ion Exchange Chromatography

Flow-through configurations render traditional chromatographic applications more efficient with higher resolution. The technique possesses advantages that suit the technique for a wide variety of applications. The enhanced mass transfer of flow-through media makes them unsuitable for most instances of gel-filtration

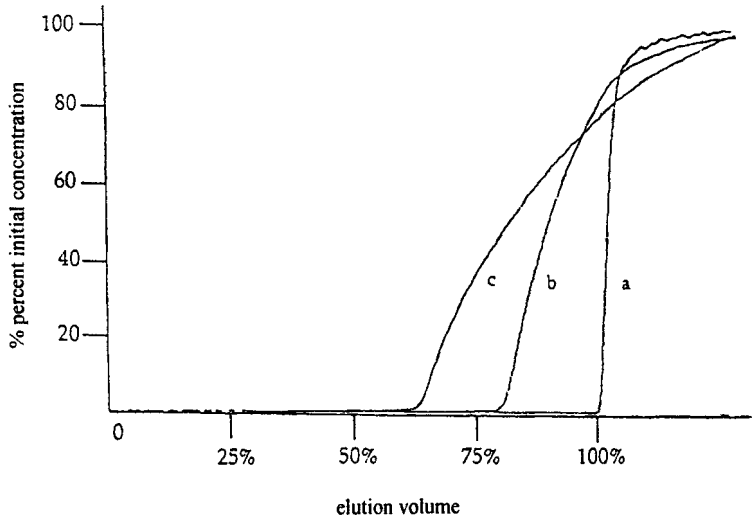

Figure 19. Solute breakthrough curve for the chromatography of bovine serum albumin on a 2.1 mm ID x 30 mm column of Mono Q (10 mm d_p and 600 Å d_{pore}) in 20 mM Tris-HCl, pH 8.0 with detection at 280 nm: a.) 50 cm/h, b.) 1000 cm/h, c.) 2500 cm/h. Reprinted with permission, J. Chromat., 512, 1 (1990). Copyright 1990, Elsevier Publ.

chromatography[17]. Insufficient "sieving" thus is typical. However media, such as HyperD, which diminish mass transfer to augment the surface area for adsorption during separation succeed in gel-filtration applications. Also ion exchange proceeds admirably. Human transferrin is acutely separated from bovine serum albumin with[12] an POROS Q/H flow-through anion exchanger in much less than 5 min.

Flow-through ion exchange separation can be even more discerning. To facilitate ion exchange fractionation[58], negatively charged tails were added to the footprint of retention for β-galactosidase. The tails consisted of polyaspartate fusions. Wild type β-galactosidase (BGWT) and four of its fusion variants (incorporating respectively one, five, eleven, and sixteen additional aspartate residues) (respectively BGCD 1, BGCD 5, BGCD 11, and BGCD 16). These were fractionated at high resolution using POROS Q/M anion exchange in 10 min. Resolution is thus not sacrificed fractionating protein molecules that differ *only* by a few charges. Retention time depends on ionic strength and similarly on pH (Figure 20). Precise results were provided for the dependence of retention on the number of displaced species and of ion exchange sites. Flow-through separations improve yield and purity, decrease process time, and process very large loading volumes. Strong cation exchange, combined with reversed-phase, flow-through chromatography of tick anticoagulant peptide (TAP) produced 12 g of TAP from 200 l of fermentation broth[59]. Moreover

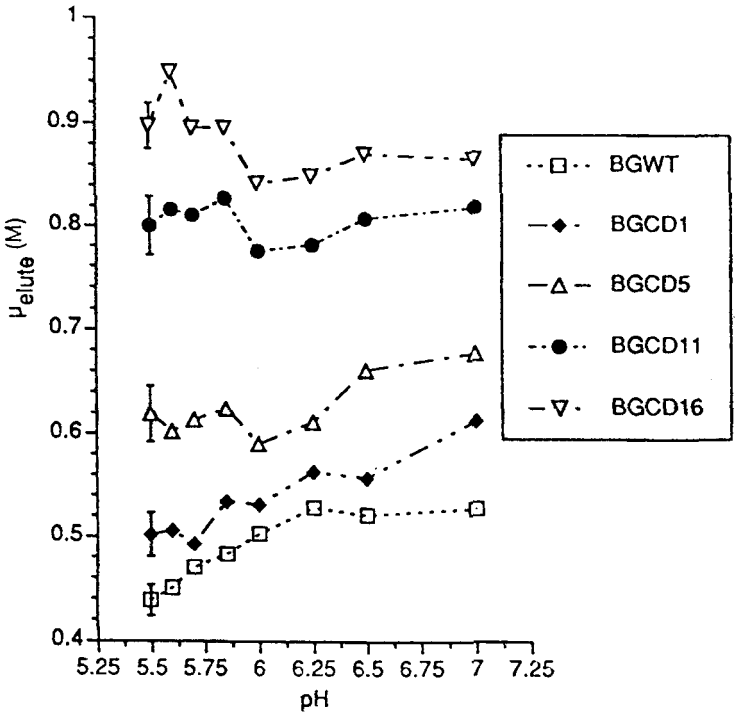

Figure 20. Protein retention (measured as the NaCl concentration required to elute the protein μ_{elute}) vs. pH for BGWT and BGCD fusions in 25 mM bis-Tris at 1 ml/min and 21° C. Each data point represents at least 3 replicates. Reprinted with permission, J. Chromat. A, 689, 227 (1995). Copyright 1995, Elsevier Publ.

TAP yield improved from 32 to 47%, process time was halved, and low-temperature processing was eliminated.

Flow-through cation exchange chromatography exploits the cationic character of some antibodies to isolate them. For example, the technique separates[60] three Fab isoforms in about 20 min. Mouse anticortisol monoclonal antibody (IgG_{2b} subclass) was raised and digested with papain to yield Fab and Fc fragments. The Fab fragments possessed pI's of 5.4, 5.5, or 5.8. A mixture of Fab fragments was applied to a POROS strong cation exchange column to which a pH gradient was applied to elute the fragments (Figure 21). Capillary electrophoresis demonstrated that each fragment was thus isolated with greater than 90% purity. Moreover the gentle elution conditions of a pH gradient ensured that each Fab fragment exhibited full biological activity after purification. Cation exchange chromatography can thus be used as an alternative to Protein A affinity chromatography. Monoclonal antibody MAb 414 was

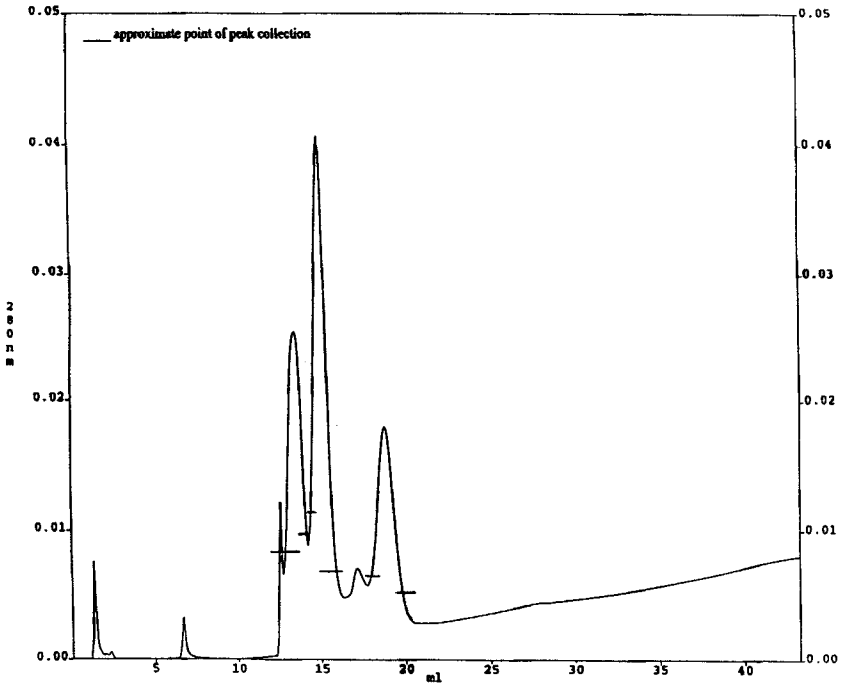

Figure 21. A_{278} vs. elution time separating Fab fragments on a strong cation exchange column (4.6 mm ID x 100 mm) of POROS (d_p 20 μm). Separation was achieved with a pH gradient. Reprinted with permission, J. Chromat. A, 707, 225 (1995). Copyright 1995, Elsevier Publ.

isolated from ascites fluid using two cation exchangers[61], columns of respectively MacroPrep high S and ceramic hydroxyapatite. Excellent resolution resulted from applying a shallow NaCl gradient, providing an alternative to Protein A chromatography able to fractionate different IgG's and separate solutes under more gentle conditions.

Reversed-Phase Chromatography

The high resolution and short elution time of flow-through chromatography makes separations convenient. For instance, the Aα, Bβ and γ chains of human fibrinogen were resolved well in 3 minutes via reversed-phase chromatography[62] (Figure 22). SDS-PAGE confirmed the excellent purity of the separated chains. The simplicity of such distinguished separation is noteworthy. This technique was ultimately used to cultivate monoclonal antibodies specific for various fibrinogen epitopes. The efficiency of flow-through reversed-phase chromatography has been exploited in the

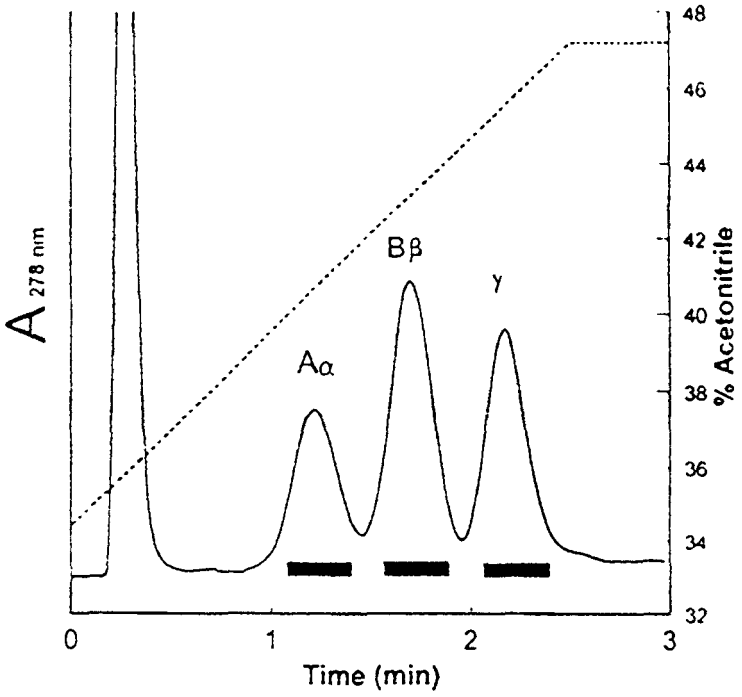

Figure 22. A_{278} vs. elution time separating the chains of reduced S-carboxymethylated human fibrinogen on POROS 20-R2. A linear gradient of 34.4-47.2% acetonitrile at a flowrate of 10 ml/min over 2.5 min was used in reversed-phase chromatography. Reprinted from Thromb. Res., 79, 405, copyright 1995, with permission from Elsevier Science Ltd., The Boulevard, Langford Lane, Kidlington OX5 1GB, UK.

dairy industry[56]. Quality control of milk products analyzes whey proteins chromatographically. The resolution of β-lactoglobulin A and β-lactoglobulin B suffered using conventional methods. Previous analysis used reversed-phase HPLC, which is limited by long analysis times and fouling. In merely 1.5 min, analysis of raw bovine milk with a reversed-phase column of POROS 1 10R resolved in 1.5 min the major whey proteins serum albumin, α-lactalbumin, β-lactoglobulin A, and β-lactoglobulin B. Excellent separation between these proteins was obtained, which was reproduced in the separation of ovine and caprine whey proteins. This study separated β-lactoglobulin types as well as species differences between α-lactalbumin. A flow-through configuration enhances the efficiency of reversed-phase chromatography, which is sensitive to fine differences in primary structure.

Frontal analysis of the reversed-phase separation of five proteins by flow-through chromatography accordingly displays negligible difference over a 170-7000 cm/h

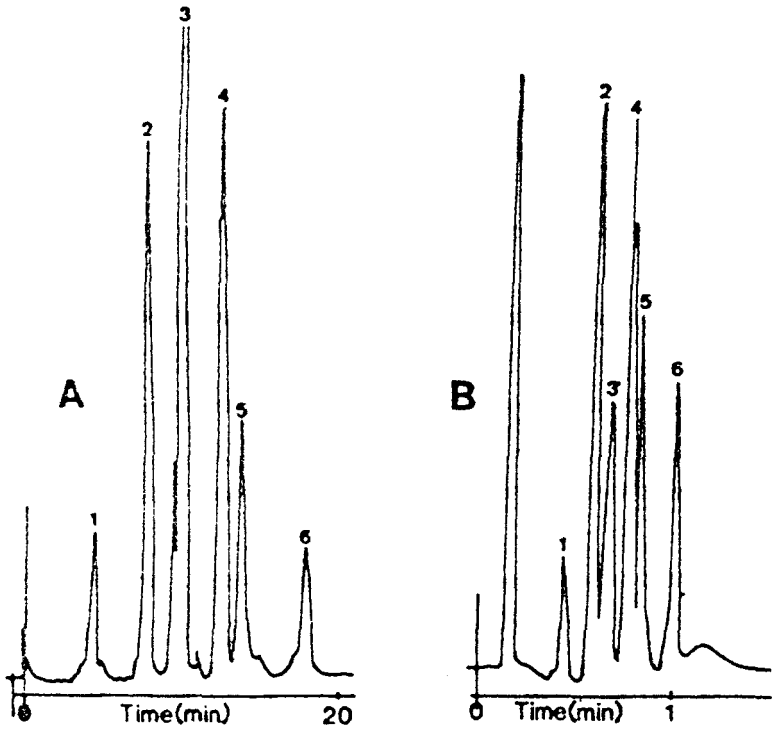

Figure 23. A_{278} vs. elution time separating six proteins on a 4.6 mm ID x 50 mm column in reversed-phase chromatography. A linear gradient of (A) 15-55% acetonitrile in 0.1% trifluoroacetic acid at a flowrate of 1 ml/min was used on PLRPS 300 Å (d_p 5 µm) or (B) 18-60% acetonitrile in 0.1% trifluoroacetic acid at a flowrate of 4 ml/min was used on PLRPS 4000 Å (d_p 8 µm). 1= ribonuclease A, 2 = cytochrome c, 3 = lysozyme, 4 = bovine serum albumin, 5 = myoglobin, 6 = ovalbumin. Reprinted with permission, J. Chromat., 512, 365 (1990). Copyright 1990, Elsevier Publ.

range of superficial velocities[31]. Sharp breakthrough curves were displayed throughout this range. Reversed-phase chromatogaphy via parallel column gradient elution was conducted in one of the first flow-through configurations[18]. Thus, in a single gradient cycle, chromatography of six globular proteins on Polymer Labs PLRP-S 1000 Å media separates them in 60 s (Figure 23). Ion exchange chromatography of adenosine 5'-monoposphate, myoglobin, and ferritin on Polymer Labs PLRP-S 4000 Å media demonstrates that speed does not reduce resolution at high flowrates. Figure 24 shows that H is independent of linear velocity above 3.5 mm/s.

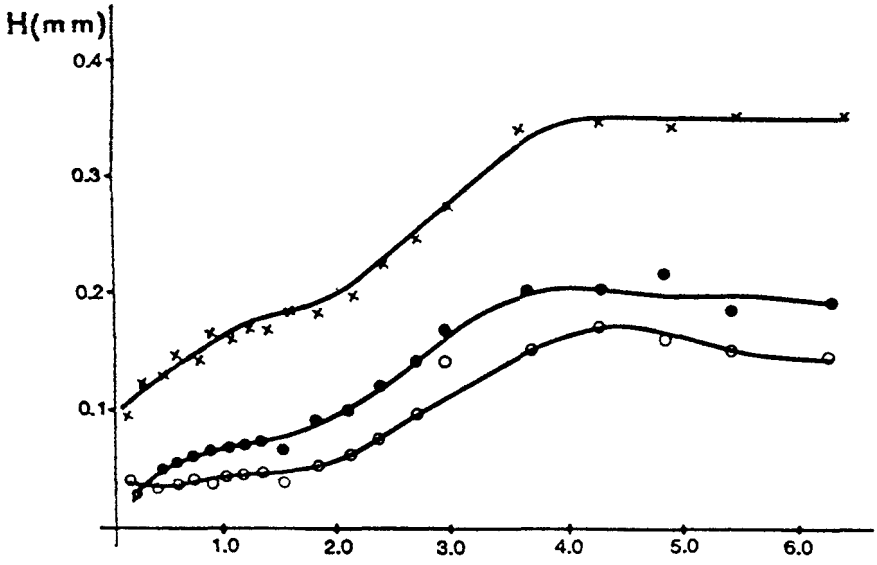

Figure 24. H vs. v_o for a 4.6 mm ID x 250 mm column of PL-SAX 4000 (d_p 8 μm) media run under no retention. The eluent is 0.01 M Tris-HCl, 0.5 M NaCl, pH 8.0 for adenosine 5'-monophosphate (O) myoglobin (●), and ferritin (X). Reprinted with permission, J. Chromat., 512, 365 (1990). Copyright 1990, Elsevier Publ.

The combination of high resolution and speed characteristic of flow-through chromatography has also found use in LC/MS analyses. For instance, reversed-phase flow-through chromatography can be used as a second chromatographic mode in two-dimensional heart-cutting systems. This combination was recently used to separate the components in *Eschericia coli* lysate[64] and characterize their molecular weight with MS. Analytically characterization was comparable to current methods such as SDS-PAGE. Flow-through separation preceding MALDI constitutes a powerful and efficient method of analysis[56].

Affinity Chromatography

The high efficiency and capacity of HyperD separation of biochemicals is very promising. Globular proteins are separated with higher throughputs though undiminished recovery compared[25] to media with the same d_p. The high capacity of these media are applied to advantage on an industrial scale, separating antithrombin III from Cohn Fraction IV-1 paste[27] using heparin-HyperD. These media exhibit promise removing solvent-detergents inactivating viruses in biological fluids[24]. Detergent removal also responds to the matrix/hydrogel ratio in the media formulation. The

advantages of HyperD suit the separation of rDNA products such as murine and human monoclonal Ab's as well as cytokines and cell growth factors[26]. The resistance of these media to oxidizing agents during washing suits industrial applications. Furthermore the media, typically implemented as ion exchangers, are nontoxic to cell cultures.

NOVEL APPLICATIONS

Flow-through media can used to separate biomolecules other than proteins. Chromatography need not be used as the means of separation. The macroporous nature of such media suits them for important batch separations. For example, the liposaccharide endotoxin of *Haemophilus influenzae* type b (Hib) was separated[65] from the Hib vaccine, a polyribosylribitol phosphate capsular polysaccharide (PRP). The vaccine for Hib is developed from cultures grown in a fermentor. The endotoxin is removed from the vaccine to reduce the pyrogenic response. One ultimately wants high vaccine yields. PRP separated from its endotoxin using HP 20, the hydrophobic PSDVB resin of Mitsubishi Kasei. Sodium deoxycholate is added to the suspension of PRP and endotoxin to break up endotoxin aggregates. The lipid endotoxin has access to the hydrophobic resin surface due to the large pore size of 400 Å and preferentially binds to the surface. 99.99% of the endotoxin was removed from the PRP, and its yield was nearly tripled, to about 90%.

Inside-out ligand attachment (IOLA) exploits principles similar those highlighted in flow-through chromatography. Prevalent in both techniques are larger particle pores to enhance intraparticle mass transport, augmenting separation. IOLA particles have been developed by LigoChem[66] possessing diameters of 0.2 to 3 mm, 4-40 times the d_p of flow-through media and 50-500 times the d_p of conventional media. Accordingly these cellulose-based hydrogels display large d_{pore}, comparable to flow-through supports. Resolution is enhanced further because affinity, ion exchange, and antibody ligands are bound to the porous surfaces of IOLA media, increasing the binding capacity for solutes.

CONCLUSIONS

Flow-through chromatography displays excellent potential in protein separations. The versatility of the technique suit widespread analytical and preparative applications. The intraparticle convection characteristic of flow-through chromatography furnishes excellent chromatographic properties and occurs when particle pore diameters are on the order of 1000 Å, better yet 10,000 Å. The effective intraparticle diffusivity of solutes is enhanced, and the height of a theoretical plate is diminished. A bimodal pore distribution can increase particle surface area. Modeling of transport phenomena in flow-through particles and columns demonstrates that intraparticle convection enhances resolution. Breakthrough behavior is also enhanced although this depends more on the particular particle and chromatography properties. The characteristics of flow-through particles result in both excellent resolution in separations demanding short elution times and the ability to process large sample volumes if flow-through particles possess large surface areas.

BIBLIOGRAPHY

1. NB Afeyan, NF Gordon, I Mazsaroff, L Varady, SP Fulton, Y-B Yang, and FE Regnier, J. Chromat., 519, 1 (1990).
2. D Schmalzing, W Nashabe, X Yao, R Mhatre, FE Regnier, NB Afeyan, and M Fuchs, Anal. Chem., 67, 606 (1995).
3. S Tsuneda, K Saito, S Furusaki, and T Sugo, J. Chromat. A, 689, 211 (1995).
29. A Seidel-Morgenstern and G Fuiochon, AIChE J., 39, 809 (1993).
4. SJ Gibbs, and EN Lightfoot, Ind. Eng. Chem. Fund., 25, 490 (1986).
5. T Orr, Genetic Engineering News, 17(1), 6 (1996).
6. JP Tharakan and M Belizaire, J. Chromat. A, 702, 191 (1995).
7. BioRad, "UNO Ion Exchange Columns," 1997.
8. KH Hamaker and MR Ladisch, Sep. and Purif. Meth., 25, 47 (1996).
9. KH Hamaker, J Liu, RJ Seely, CM Ladisch and MR Ladisch, Biotechnol. Prog., 12, 184 (1996).
10. Y Yang, A Velayudhan, CM Ladisch and MR Ladisch, J. Chromat., 598, 169 (1992).
11. AE Rodrigues, LC-GC Int., 6(1), 20 (1993).
12. NB Afeyan, SP Fulton, and FE Regnier, J. Chromat., 544, 267 (1991).
13. F Svec and JMJ Frechet, Science, 273, 205 (1996).
14. L Varady, N Mu, Y-B Yang, SE Cook, NB Afeyan and FE Regnier, J. Chromat., 631, 107 (1993).
15. W Muller, J. Chromat., 510, 133 (1990).
16. KK Unger, R Kern, MC Ninov and K-F Krebs, J. Chromat., 99, 435 (1974).
17. PerSeptive BioSystems, "The Busy Researcher's Guide to Biomolecule Chromatography," 1996.
18. G Thevenon-Emeric and FE Regnier, Anal. Chem., 63, 1114 (1991).
19. LL Lloyd and FP Warner, J. Chromat., 512, 365 (1990).
20. Pharmacia RESOURCE flyer (1994).
21. GA Heeter and AI Liapis, J. Chromat. A, 743, 3 (1996).
22. GA Heeter and AI Liapis, J. Chromat. A, 776, 3 (1997).
23. Vydac, "Principles and Applications of High Performance Ion Exchange Chromatography for Bioseparations," 1996.
24. L Guerrier, I Flayeux, E Boschetti and M Burnouf Radosevich, J. Chromat. B, 664, 119 (1995).
25. E Boschetti, L Guerrier, P Girot and J Horvath, J. Chromat. B, 664, 225 (1995).
26. A Jungbauer and E Boschetti, J. Chromat. B, 662, 143 (1994).
27. WR Lebing, DJ Hammond, JE Wydick and GA Blombach, Vox. Sang., 67, 117 (1994).
28. BioRad Technical Bulletins 1842 and 1927, 1995.
29. Qiagen Inc., "Product Profile," December 1995.
30. P Gustavsson and P Larsson, J. Chromat. A, 734, 231 (1996).
31. SP Fulton, NB Afeyan, NF Gordon, and FE Regnier, J. Chromat., 547, 452 (1991).
32. R Freitag, D Frey, and C Horvath, J. Chromat. A, 686, 165 (1994).

33. A Siedel-Morgenstern and G Fuiochon, AIChE J., 39, 809 (1993).
34. Boehringer Mannheim, "Introduction to Perfusion Chromatography," 1996.
35. SJ Gibbs, EN Lightfoot, and TW Root, J. Phys. Chem., 96, 7458 (1992).
36. SM Fields, Anal Chem., 68, 2709 (1996).
37. NB Afeyan, NF Gordon, and FE Regnier, Nature, 358, 603 (1992).
38. AE Rodrigues, JM Loureiro, C Cenou, and M Rendueles d la Vega, J. Chromat. B, 664, 225 (1995).
39. JF Pfeiffer, JC Chen and JT Hsu, AIChE J., 42, 932 (1996).
40. Tom Orr, Genetic Engineering News, 16(18), 9 (1996).
41. CM Guttman and EA DiMarzio, Macromol., 3, 681 (1970).
42. O Chiantore and M Guaita, J. Liq. Chromat., 5, 643 (1982).
43. ME van Kreveld and N van Den Hoed, J. Chromat., 149, 71 (1978).
44. D Frey, E Scheinheim, and C Horvath, Biotech. Prog., 9, 273 (1993).
45. AE Rodrigues, AMD Ramos, JM Loureiro, M Diaz, and ZP Lu, Chem. Eng. Sci., 47, 4405 (1992).
46. AE Rodrigues, L Zuping, and JM Loureiro, Chem. Eng. Sci., 46, 2765 (1991).
47. G Stephanoupoulos and K Tsiveriotis, Chem. Eng. Sci., 44, 2031 (1989).
48. AI Liapis and MA McCoy, J. Chromat. A, 599, 87 (1992).
49. GA Heeter and AI Liapis, J. Chromat. A, 761, 55 (1997).
50. AI Liapis and MA McCoy, J. Chromat., 548, 25 (1991).
51. AI Liapis and MA McCoy, J. Chromat. A, 660, 85 (1994).
52. AI Liapis, Y Xu, OK Crosser, and A Tongta, J. Chromat. A, 702, 45 (1995).
53. Y Xu and AI Liapis, J. Chromat. A, 724, 13 (1996).
54. GA Heeter and A Liapis, J. Chromat. A, 734, 105 (1996).
55. GA Heeter and AI Liapis, J. Chromat. A, 760, 3 (1997).
56. PerSeptive Biosystems, "Protein Purification and Characterization: Essential Techniques for Drug Discovery and Development," 1997.
57. M McCoy, K Kalghatgi, FE Regnier and N Afeyan, J. Chromat. A, 743, 221 (1996).
58. MH Heng and CE Glatz, J. Chromat. A, 689, 227 (1995).
59. ED Lehman, JG Joyce, DK Freymeyer, J Bailey, WK Herber, and WJ Miller, Bio/Technol., 11, 207 (1993).
60. R Mhatre, W Nashabeh, D Schmalzing, X Yao, M Fuchs, D Whitney, and FE Regnier, J. Chromat. A, 707, 225 (1995).
61. JE Machamer, AJ Stapleton, T King, and K Balakrishnan, "Optimizing Antibody Purification," presented at the March 1996 ACS meeting, New Orleans.
62. S Raut, PH Corran, and PJ Gaffney, Thromb. Res., 79, 405 (1995).
63. M Torre, ME Cohen, N Corzo, MA Rodriguez and JC Diez-Masa, J. Chromat. A, 729, 99 (1996).
64. GC Opiteck, KC Lewis, and JW Jorgenson, Anal Chem., 69, 1518 (1997).
65. MS Rienstra, EM Scattergood and RD Sitrin, in "New Developments in Bioseparations," MM Ataai and SK Sikdar, eds., AIChE Symp. Ser., vol. 88, number 290, 1992, p. 52.
66. V Glaser, Genetic Engineering News, 16(12), 12 (1996).